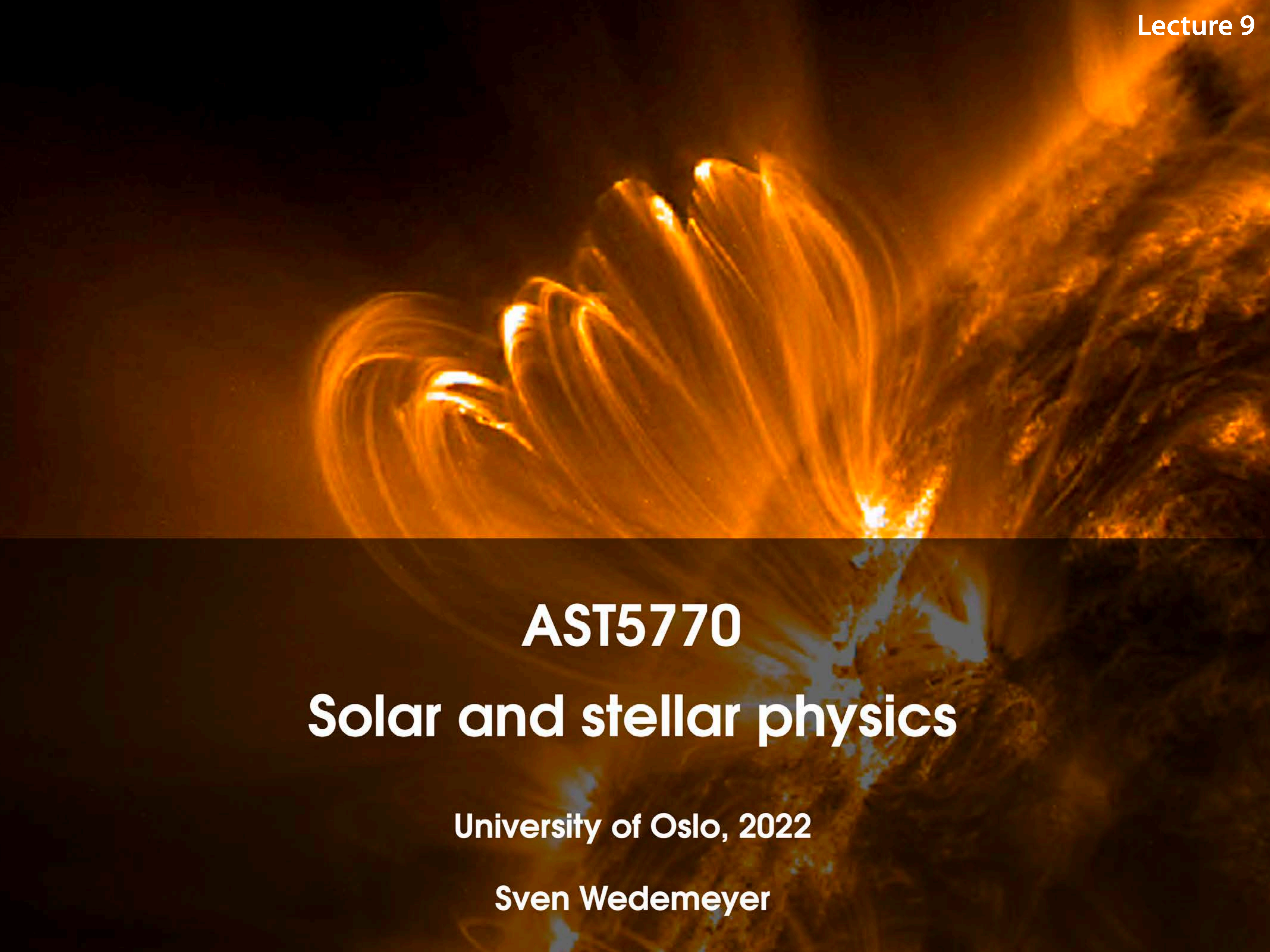

AST5770

Solar and stellar physics

University of Oslo, 2022

Sven Wedemeyer

Convection

- Convection zone: Mass density, pressure change by orders of magnitudes
- Pressure scale height for a stratified medium!

$P(z) = P_0\, e^{-(z/H_P)}$ $z = r$ *(vertical/radial coordinate)*

➡ Sets dominant spatial scale of convective motions (and convection cell sizes)

➡ Diverging upflows turn over within 1-2 scale heights, cover 2/3 of the area

➡ Downflows get compressed, fast and turbulent, occupy 1/3 of the area

- **At surface:** isolated upflows form **granules**, surrounded by connected downflows (**intergranular lanes**)

surface — photosphere seen from top

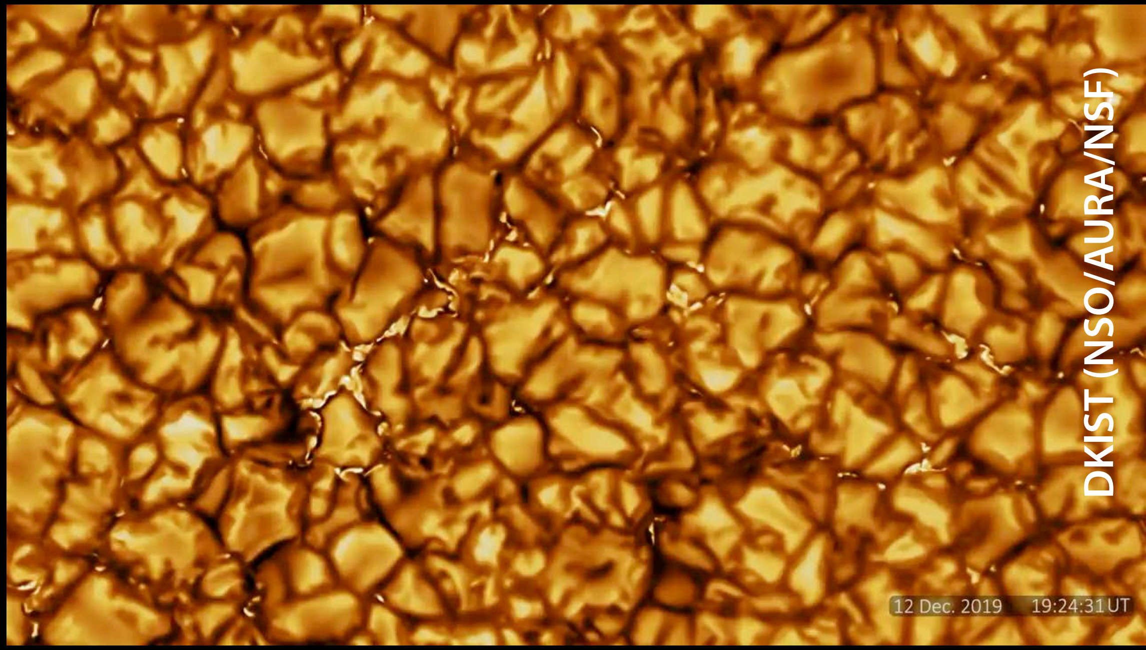

Vertical cross-section from simulation

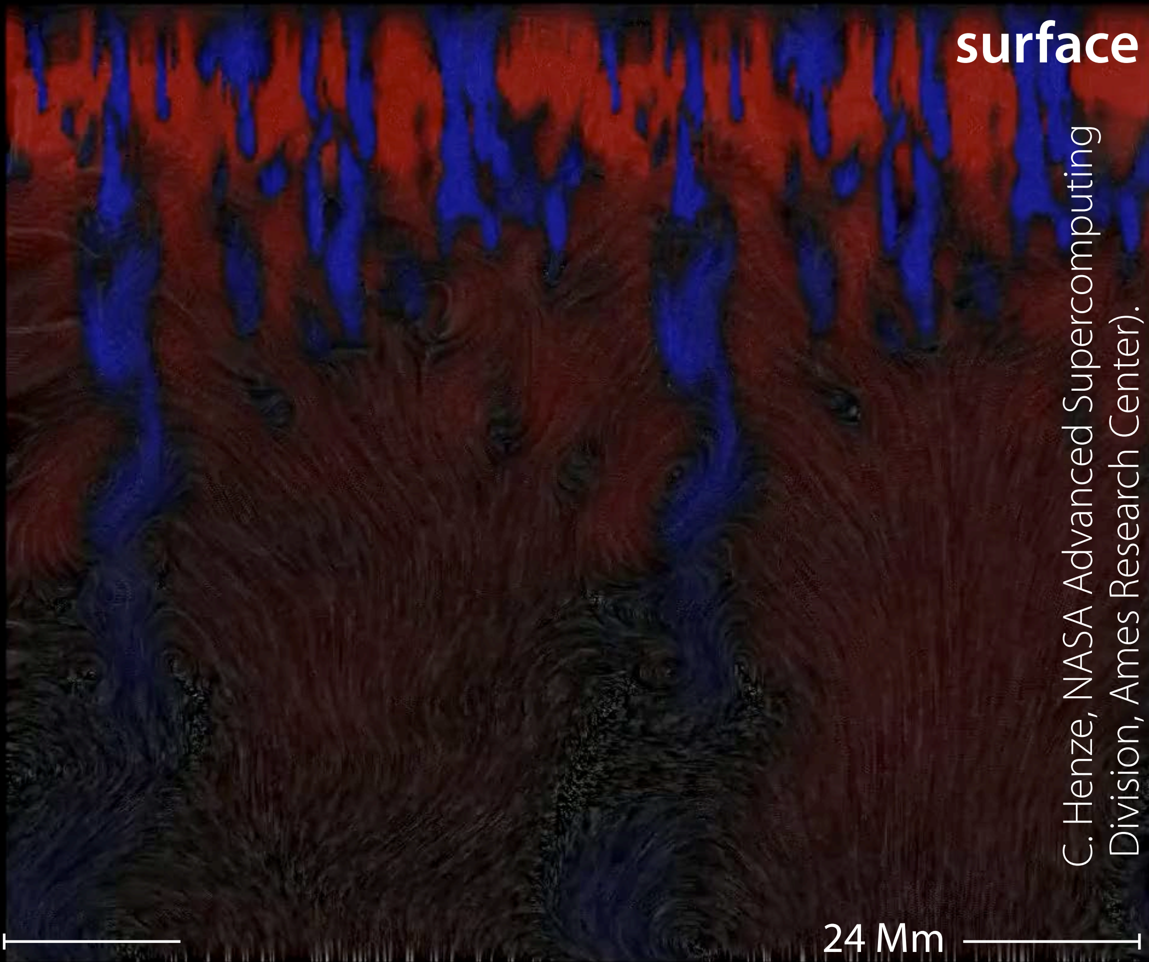

Convection

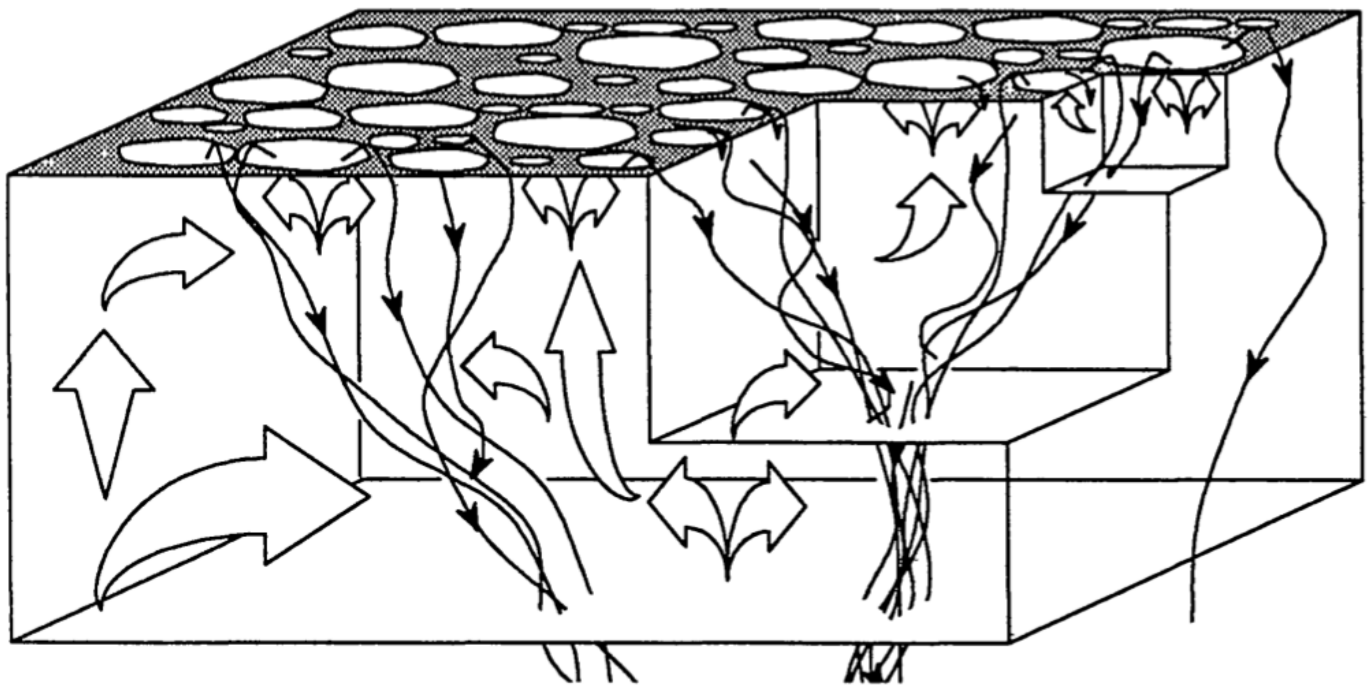

Figure 7 Flow lines showing the merging of the downdrafts on successively larger scales (schematic). The boxes cut out illustrate how the same process occurs on (in this illustration) three different scales.

surface — photosphere seen from top

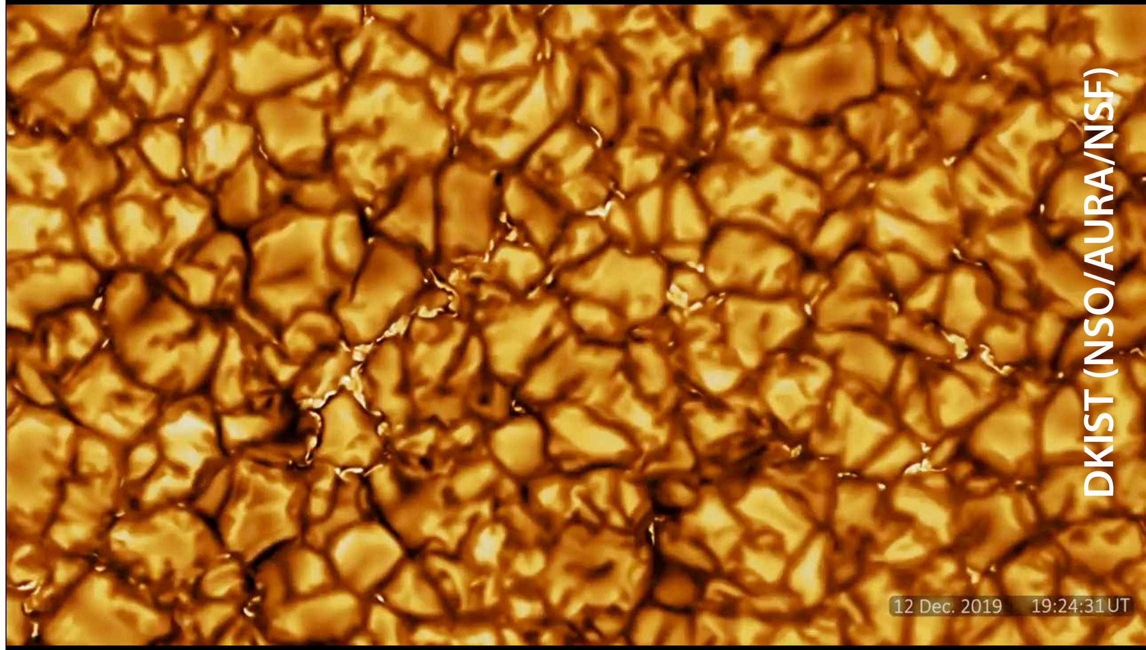

Vertical cross-section from simulation

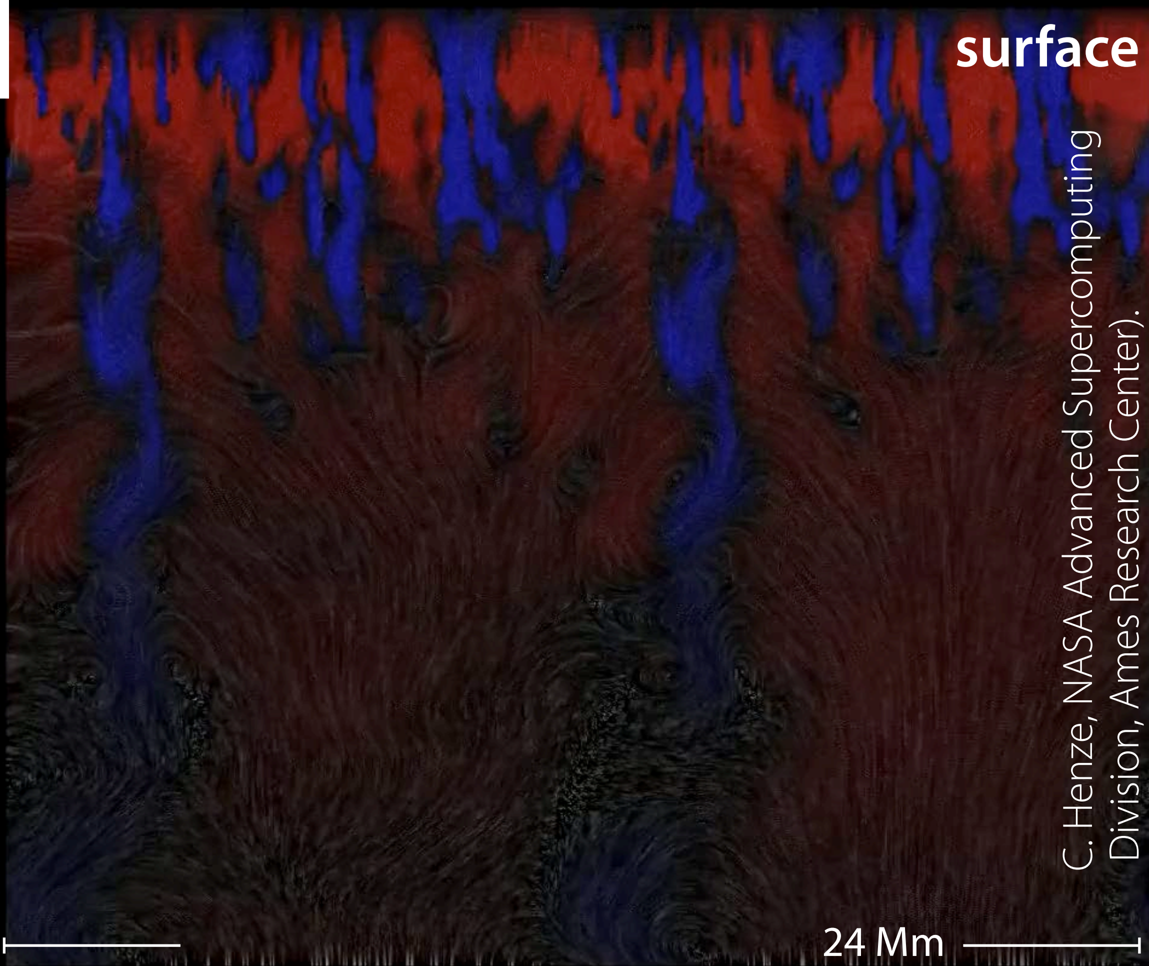

- **At surface:** isolated upflows form **granules**, surrounded by connected downflows (**intergranular lanes**)
- **Downflows merge** with each other (Spruit et al. 1990)
- The deeper, the fewer (combined) downflows
- At greater depths:
  Downdrafts in mesh-like pattern with larger diameters, eventually outlining supergranular scales.

Surface convection

Recap — Spatial scales

- Spatial power spectra reveal particular spatial scales imprinted by the Sun's convection on the surface
- **Granulation** (1-2Mm, 8-10min)
- **Supergranulation** (typically 30-40Mm, ~40h)
- Indications for giant cells (>100 Mm)
- Existence of mesogranulation (between granulation and super granulation) uncertain, debated

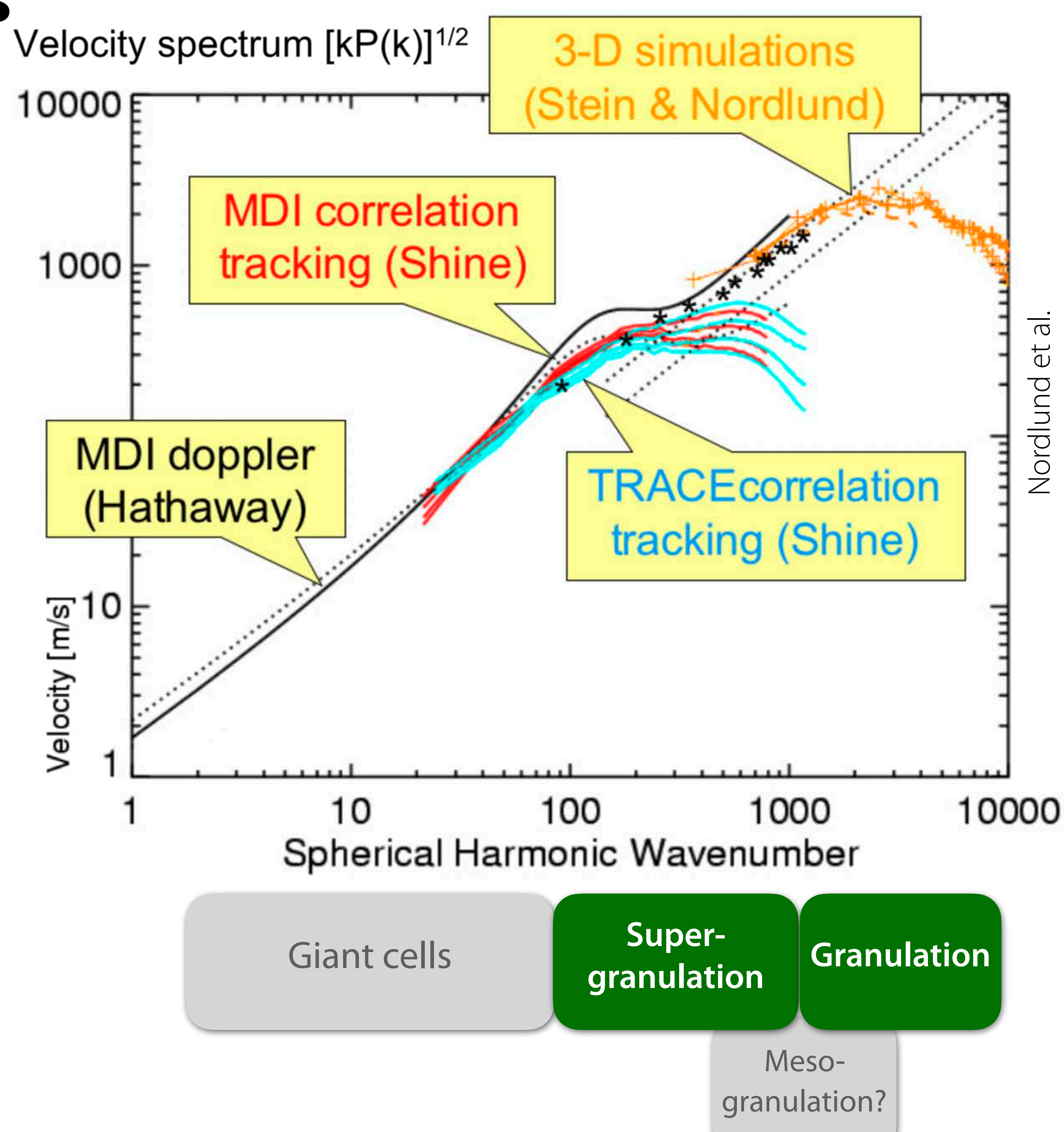

Convection

Observational indicators of convection on other stars

1. Spectral line broadening (macroturbulence)

- Stellar discs cannot be resolved (except for the Sun and some giant stars, marginally)
  ➡ How to detect if a star (point source) exhibits surface convection?
- **Spectral lines** provide information but "integrated" over the whole (unresolved) stellar disc
- Velocities of the surface flows (in the granulation) produce Doppler shifts

➡ **Spectral lines** formed in the (low) photosphere get **broadened** accordingly

- Called **macroturbulence**
- This effect is larger than broadening due to thermal motions and (non-radial) oscillations for most stars;
  Doppler shifts due to stellar rotation can (often) be separated from macroturbulence (via Fourier techniques)

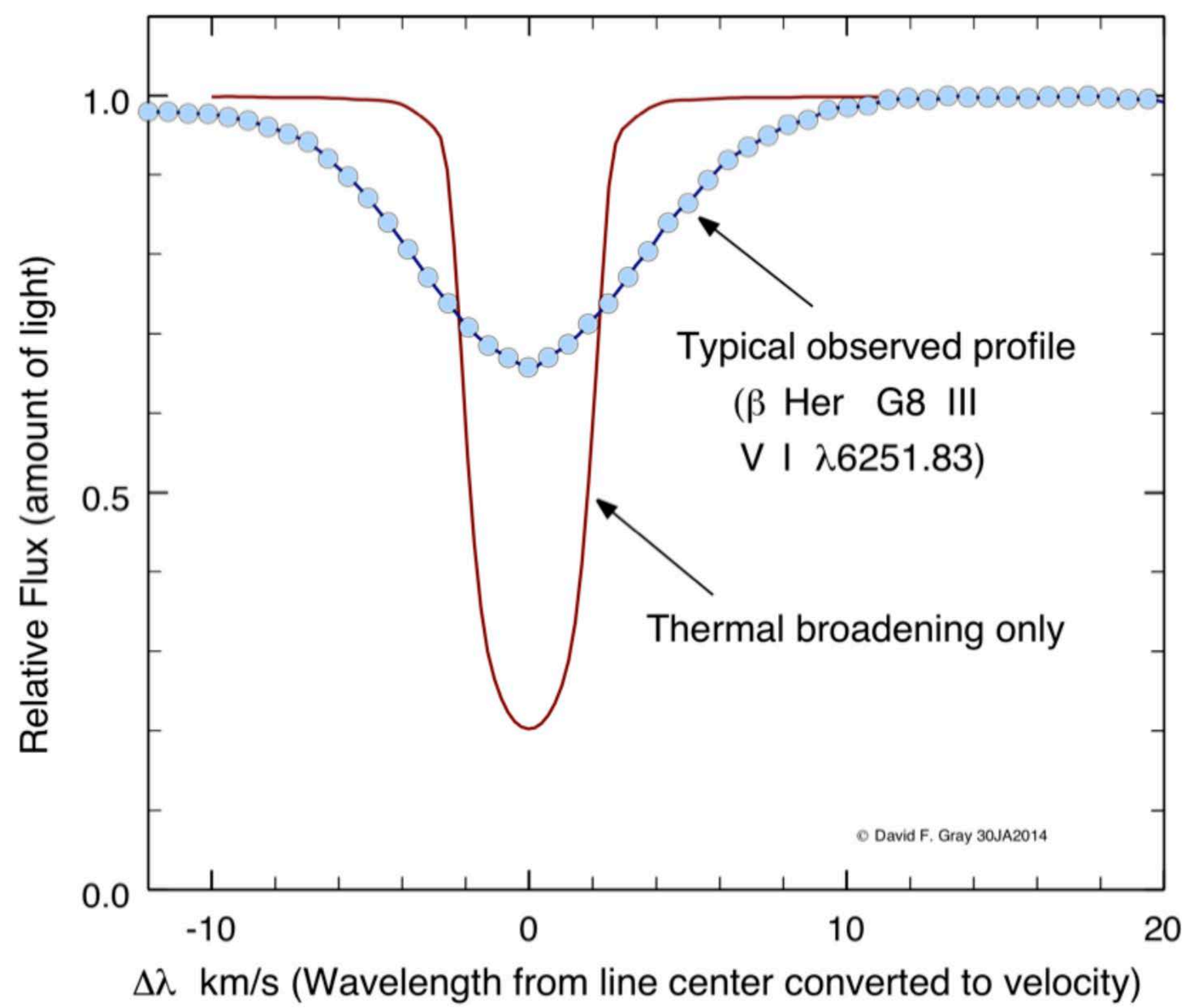

Convection

Observational indicators of convection on other stars

2. Spectral line asymmetry

- Rising gas in granules produce blueward Doppler shifts
- Sinking gas in inter granular lanes produce redward Doppler shifts
- Contributions from granules dominate (cover larger area and brighter)

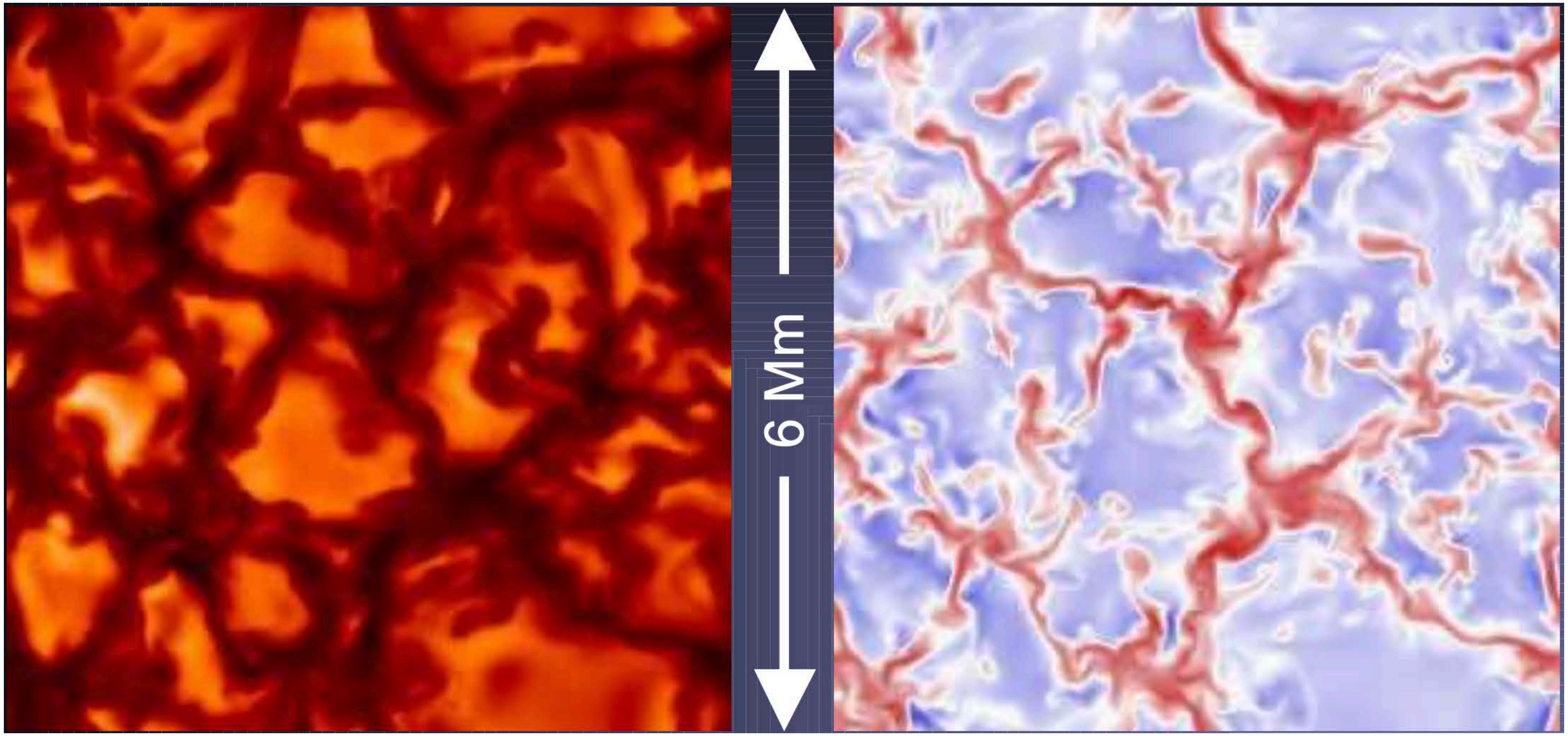

Intensity Doppler shift

3D simulation (MuRAM)

Convection

Observational indicators of convection on other stars

2. Spectral line asymmetry

- Rising gas in granules produce blueward Doppler shifts
- Sinking gas in inter granular lanes produce redward Doppler shifts
- Contributions from **granules dominate** (cover larger area and brighter)
- Combined photospheric spectral line profiles (integrated over stellar disc) are **asymmetric**

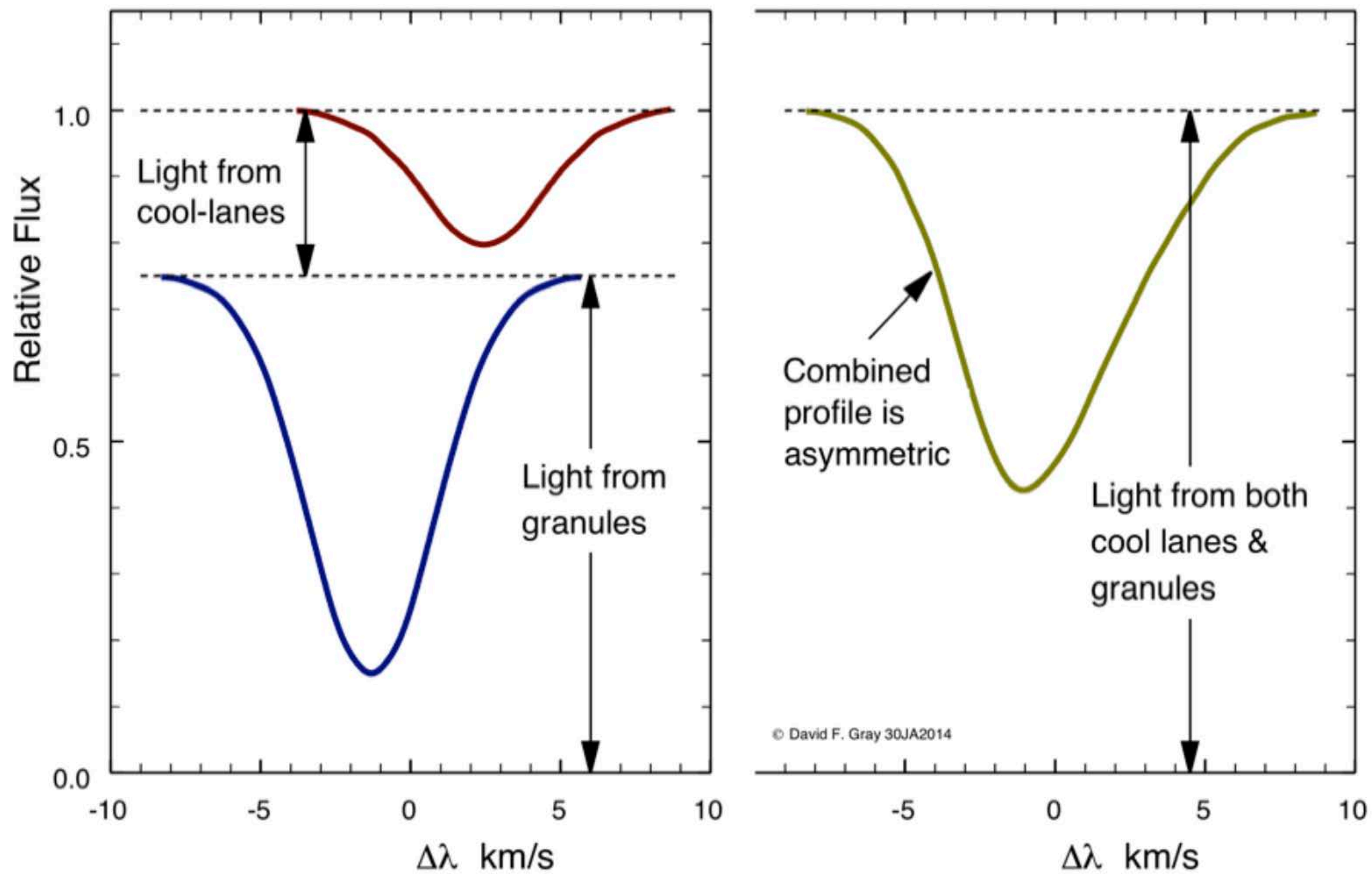

Convection

Observational indicators of convection on other stars

2. Spectral line asymmetry — line bisectors

- Spectral line asymmetries measured as **line bisector**
  - Determine midpoints between points at equal intensity level in the two line wings
  - Gives the relative shift of the midpoint for different parts of the spectral line

- Shifts can be subtle
- Bisector on the left looks almost like a straight vertical line.
- Right plot on smaller axis range reveals a C-shaped bisector

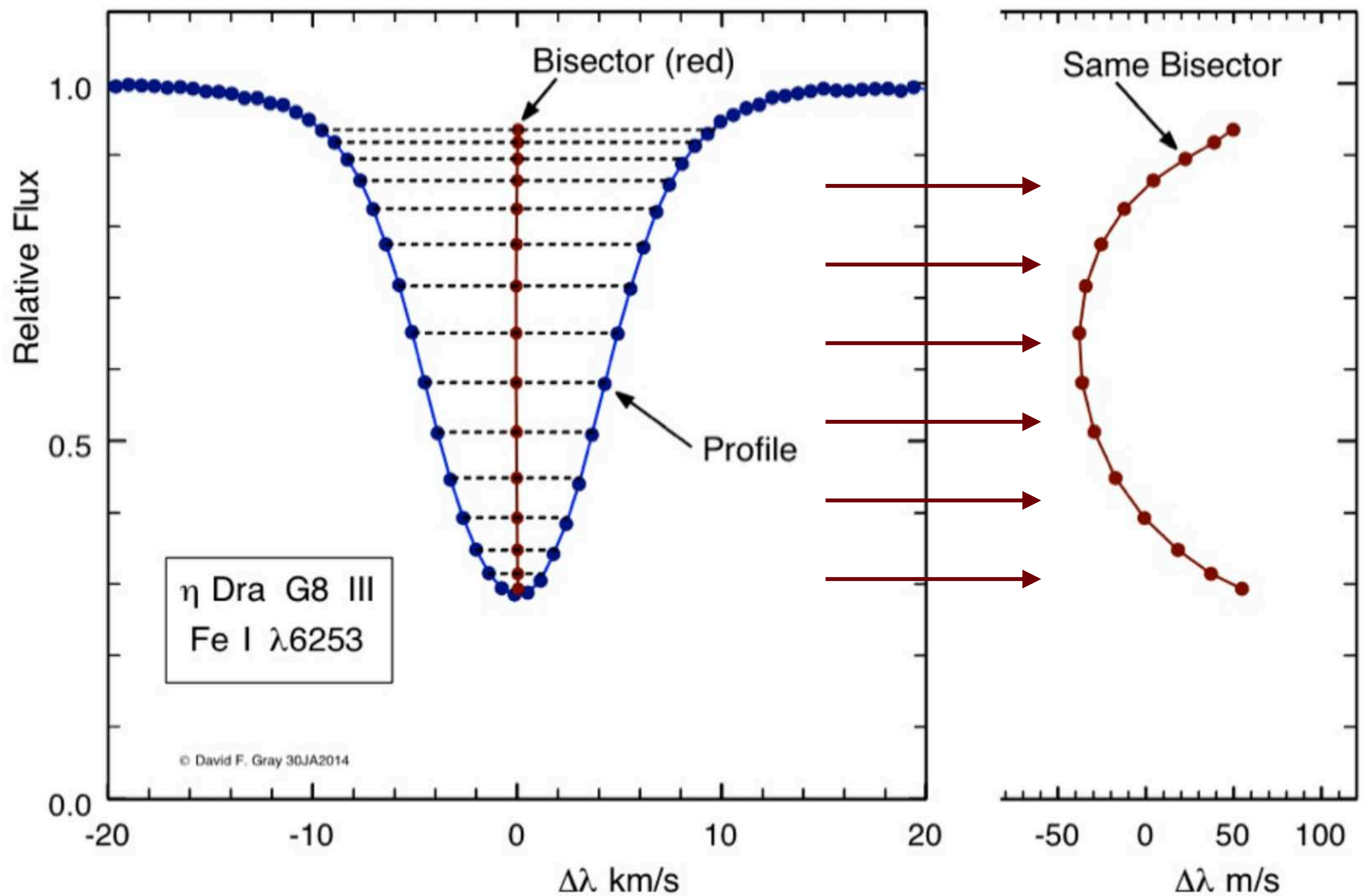

Convection

Observational indicators of convection on other stars

2. Spectral line asymmetry — line bisectors

- Cool stars (solar-like and low mass) typically exhibit C-shaped bisectors
- Reversed C-like shapes found for hotter stars (explained by Gray 2010ApJ…721..670G as normal continuation of observational granulation imprint along the main sequence)

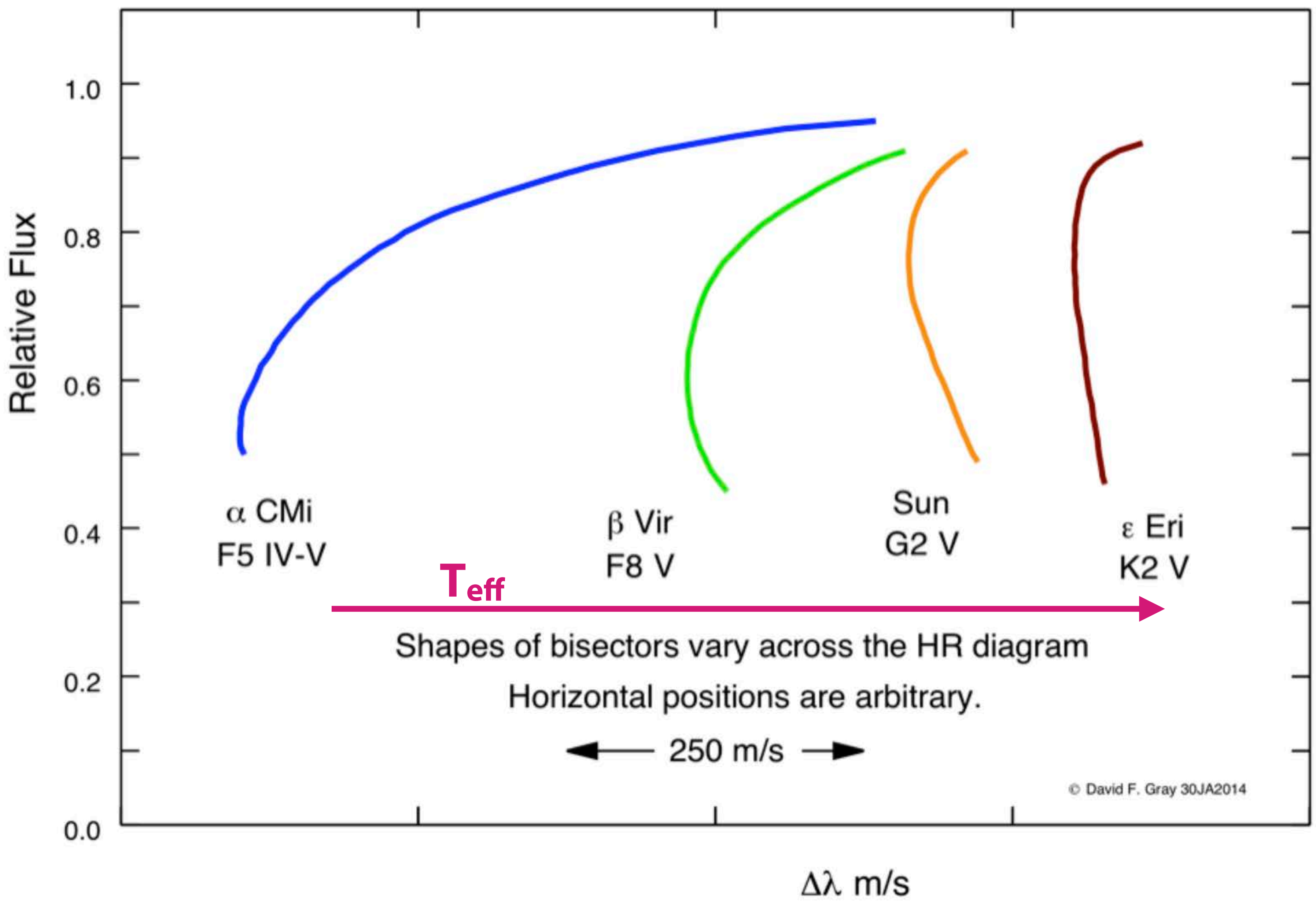

Convection

Observational indicators of convection on other stars

3. Spectral line strength — probed atmospheric layer

- Cores of weaker spectral lines are formed deep down in the stellar photosphere
- Cores of stronger spectral lines are formed higher in the stellar photosphere

Consider opacity along line of sight

- Means of probing different layers and thus the vertical velocity profile across the low photosphere and the convective overshoot region

Observations of a combination of weak and strong photospheric lines and analysis of broadening and bisectors provide important constraints for the **properties of the granulation on a star**

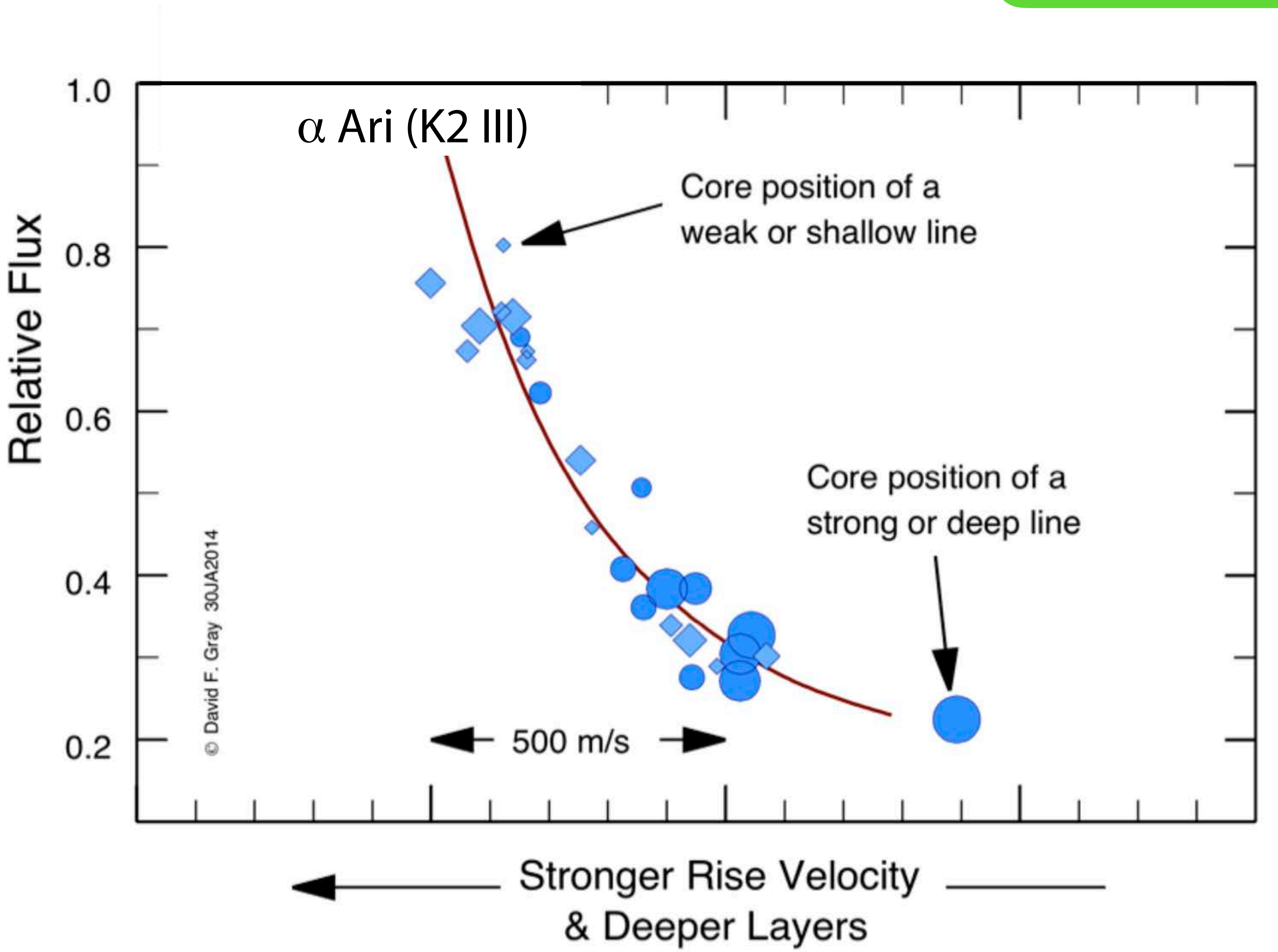

Convection

Observational indicators of convection on other stars

- Also for the Sun
  (lower angular resolution in the past)
- Comparison between observed and computed bisectors for different spectral lines with different strengths

➡ Comparison with models help to interpret the bisectors and thus derive the properties of the granulation

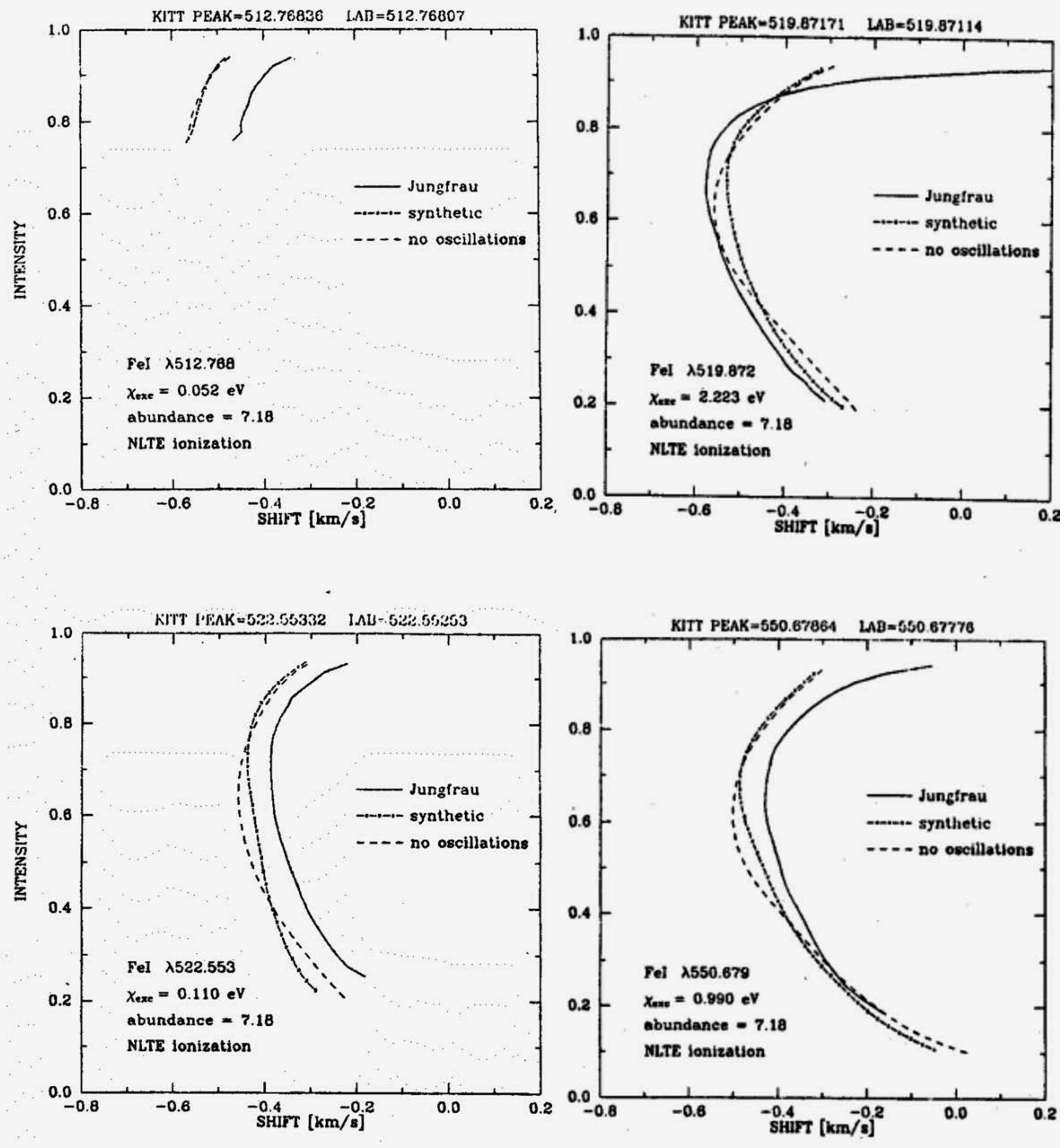

Surface convection

Granulation on other stars

(More) massive stars (M>M⊙)

Outer radiative zone, no surface convection

Spectral types A, F

- exhibit inverse bisectors
- granulation has different geometry

Solar-like and low-mass stars
Spectral types F, G, K & M

- outer convection zones and
- exhibit observable signs of convection

(Cooler) White Dwarfs

- exhibit observable signs of convection

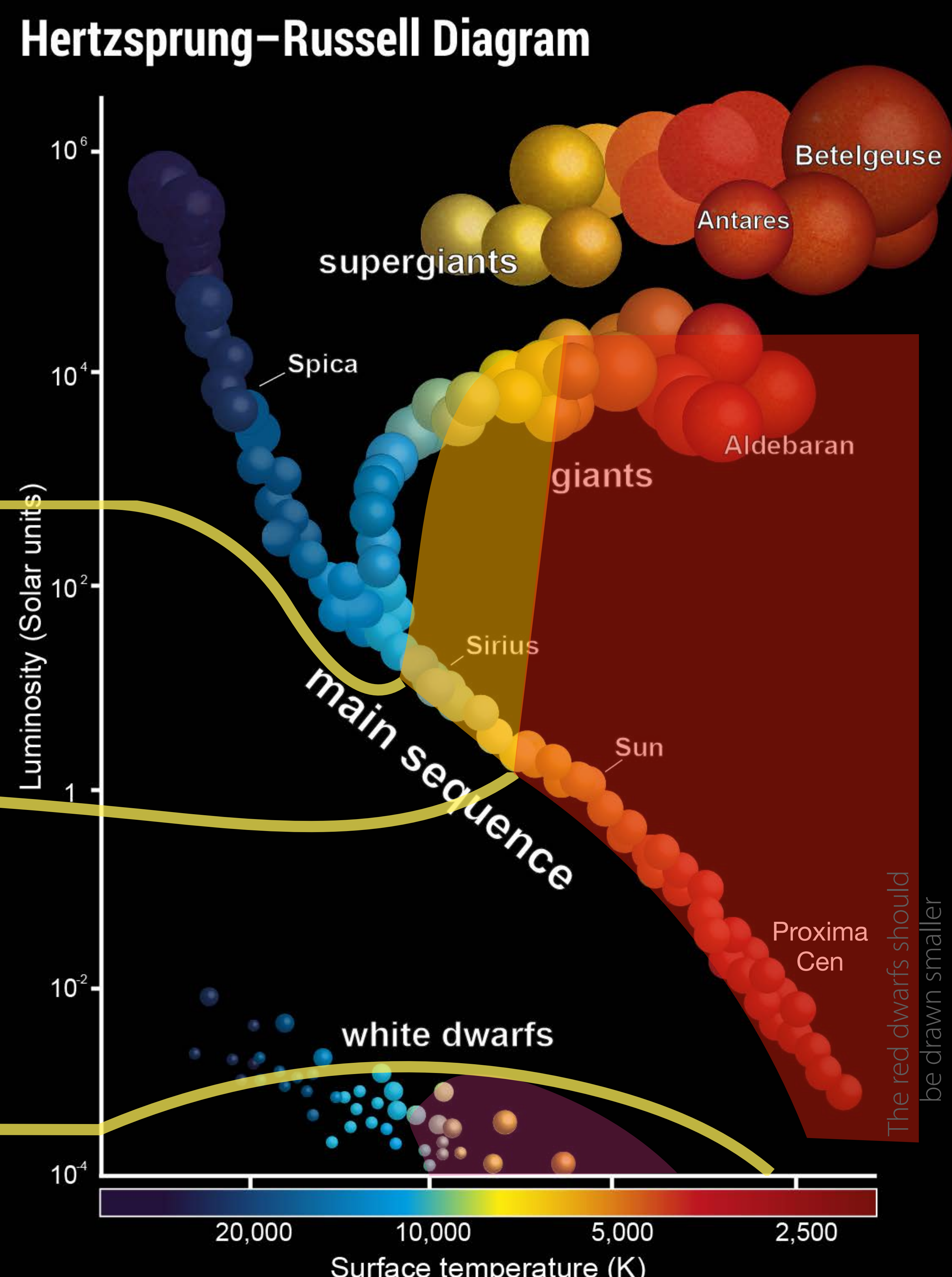

LIVERPOOL JOHN MOORES UNIVERSITY

www.schoolsobservatory.org

Surface convection

Granule sizes on other stars

- Size of granules (at the surface!) seems to scale with pressure scale height for different stellar types
- Typical granulation size determined from 3D simulations for different stellar types (Freytag et al. 2002):

$$\frac{x_{\text{gran}}}{R_*} \approx 0.0025 * \frac{R_*}{R_\odot} \frac{T_{\text{eff},*}}{T_{\text{eff},\odot}} \frac{M_\odot}{M_*}$$

  - Sun: $x_{\text{gran}} = 0.0025\, R_\odot \approx 2000$ km

- **Note:** $x_{\text{gran}} \ll R_\odot$ and turnover timescales change by 4 orders of magnitude
- Simulations of the whole convection computationally very challenging

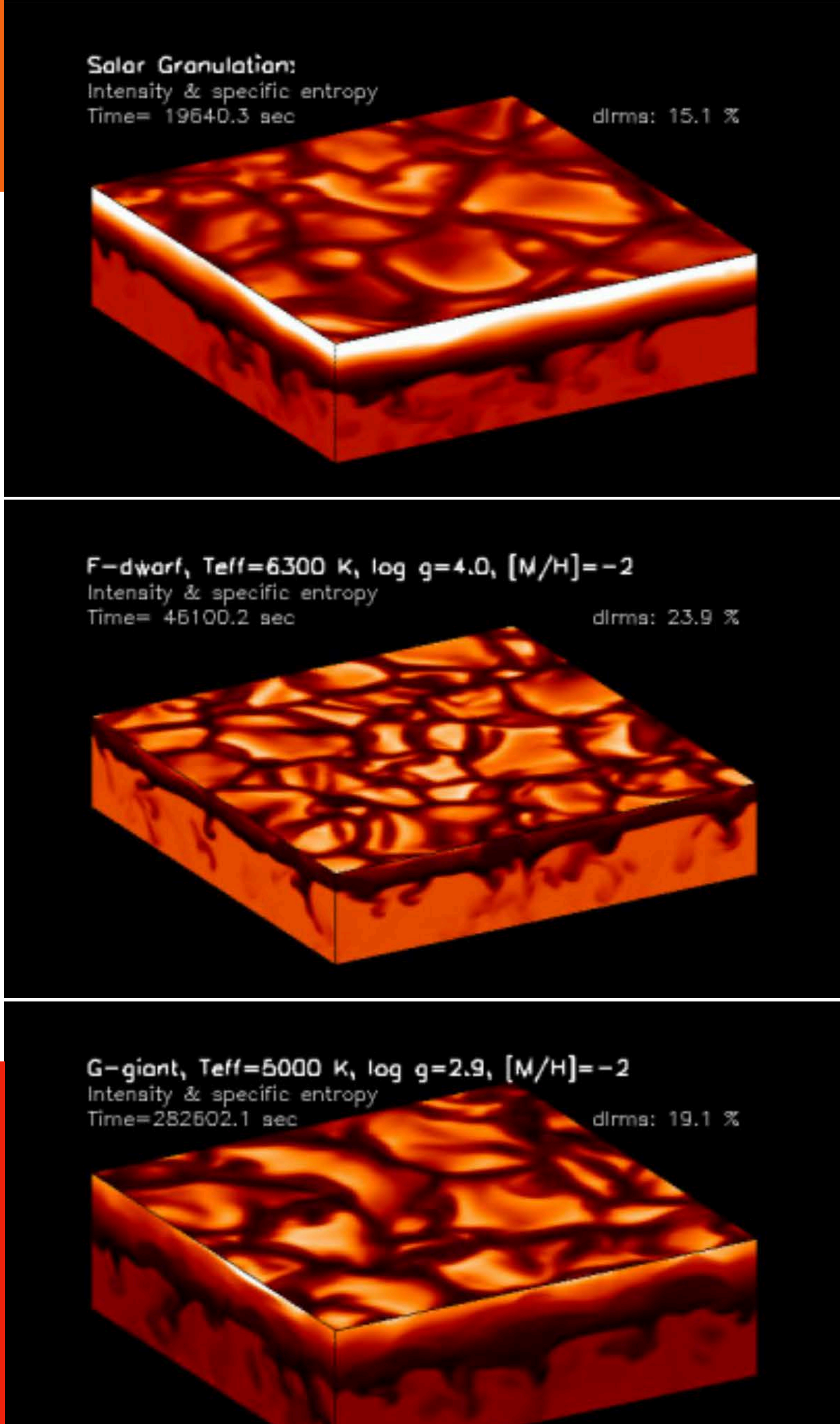

Freytag et al (2002)

Surface convection

Convection

Time-dependent 3D hydrodynamic simulation of **Betelgeuse**, here **intensity**

- Large convection cells
- Slower temporal evolution (Note time at top right)

- Observations of Betelgeuse: variations of radial velocity imply existence of large convection cells.

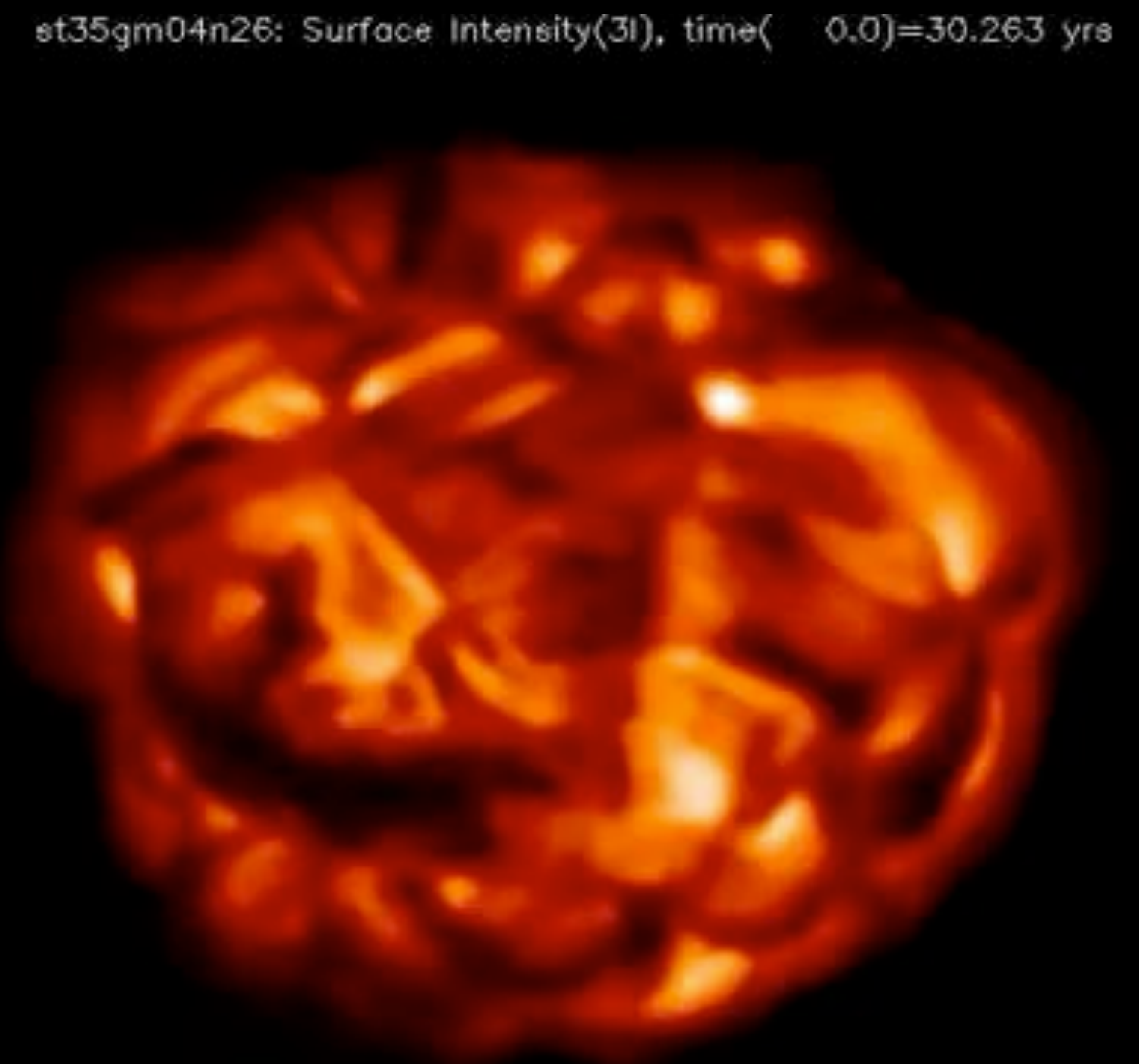

Freytag

Simulation produced with the same code as the models for the project assignment (Freytag et al. 2012)

Granulation

Granule evolution

"Birth"	"Evolution"	"Death"
• **Appearing** as initially small features	**Growing** larger in size until … • … stopping to grow, start shrinking and fading (within 5-10 min)…	• **Dissolving** (mostly smaller granules): Gets fainter and smaller until disappeared
• **Splitting** off larger granules	• … becoming unstable and splitting	• **Splitting** (large granules) into two smaller granules

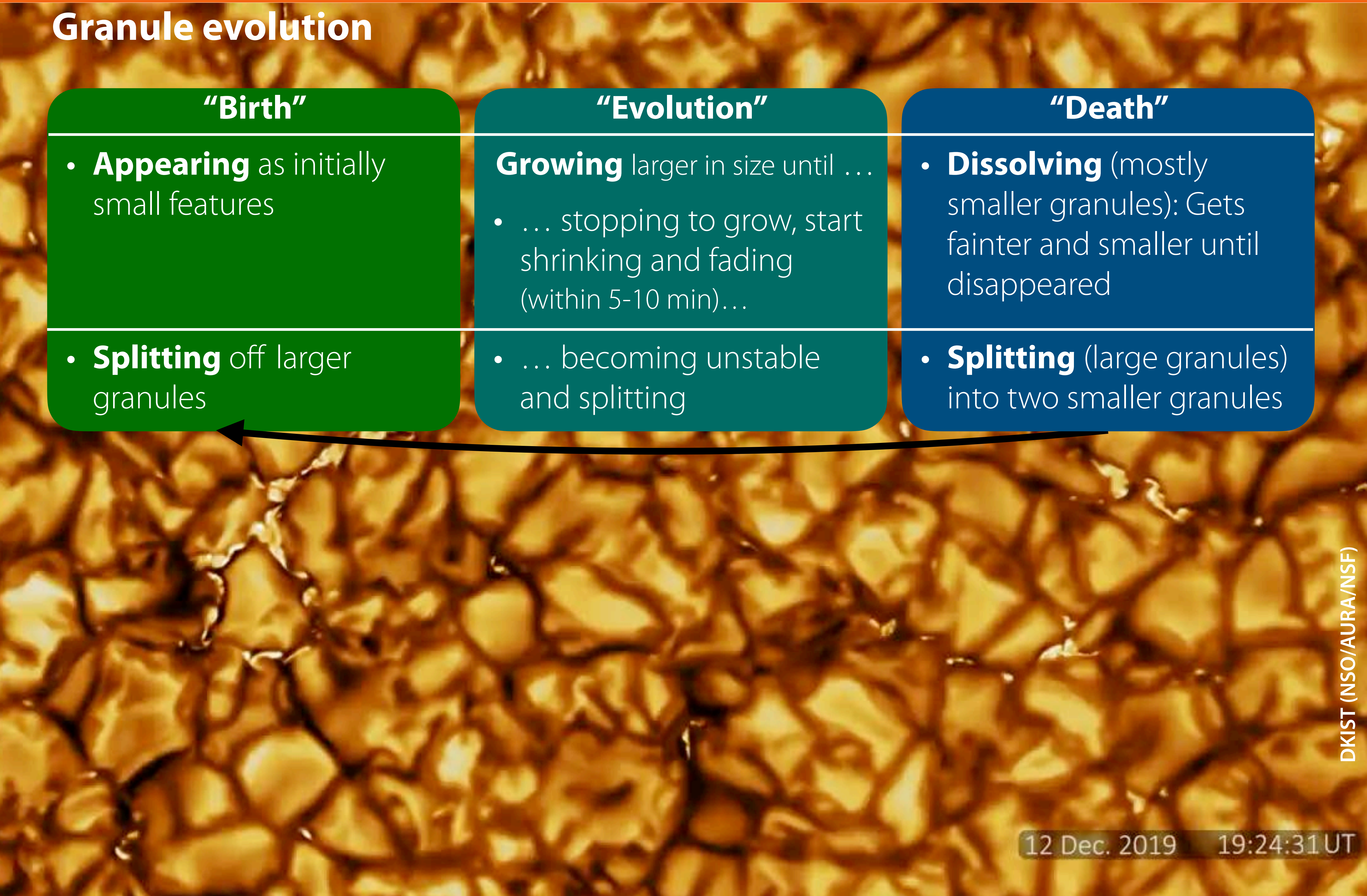

Granulation

Granule fragmentation

- Upflow leads to increased pressure and density in the granule centre

➡ Pressure gradient with respect to radiatively cooled sides

➡ Lateral (horizontal) flow of gas, diverging

- Mass conservation:

➡ Larger granules build up a larger pressure above its centre as more mass needs to be accelerated horizontally.

➡ While growing in size, pressure becomes so large that the upflow from below becomes hampered (buoyancy becomes negative, not enough energy flux to sustain luminosity at surface), while gas continues to being cooled radiatively

➡ New downflow lane forms at the granule centre

➡ The granule splits.

  - Also referred to as *"exploding granules"*

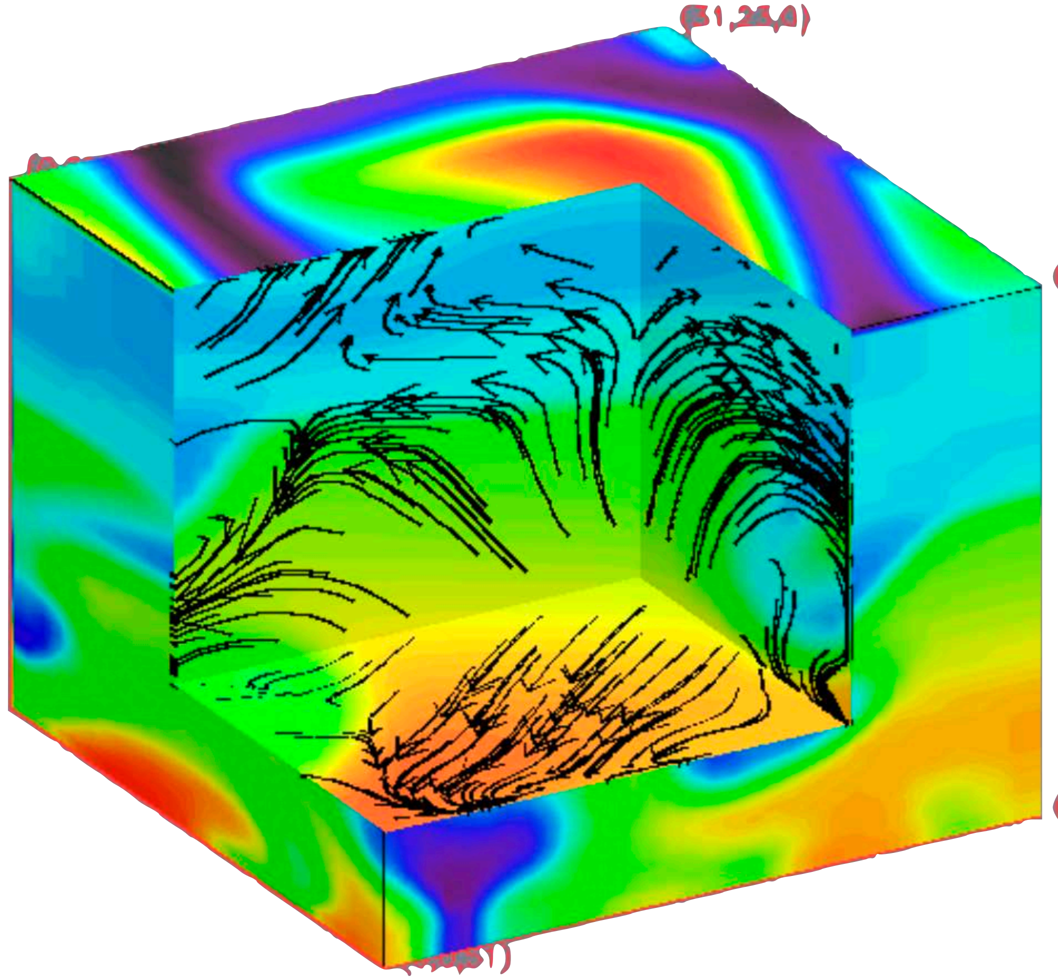

Close-up region from a 3D simulation showing gas temperature and streamlines inside and above a granule (Stein & Nordlund 1998)

Helioseismology

Helioseismology

Photospheric oscillations

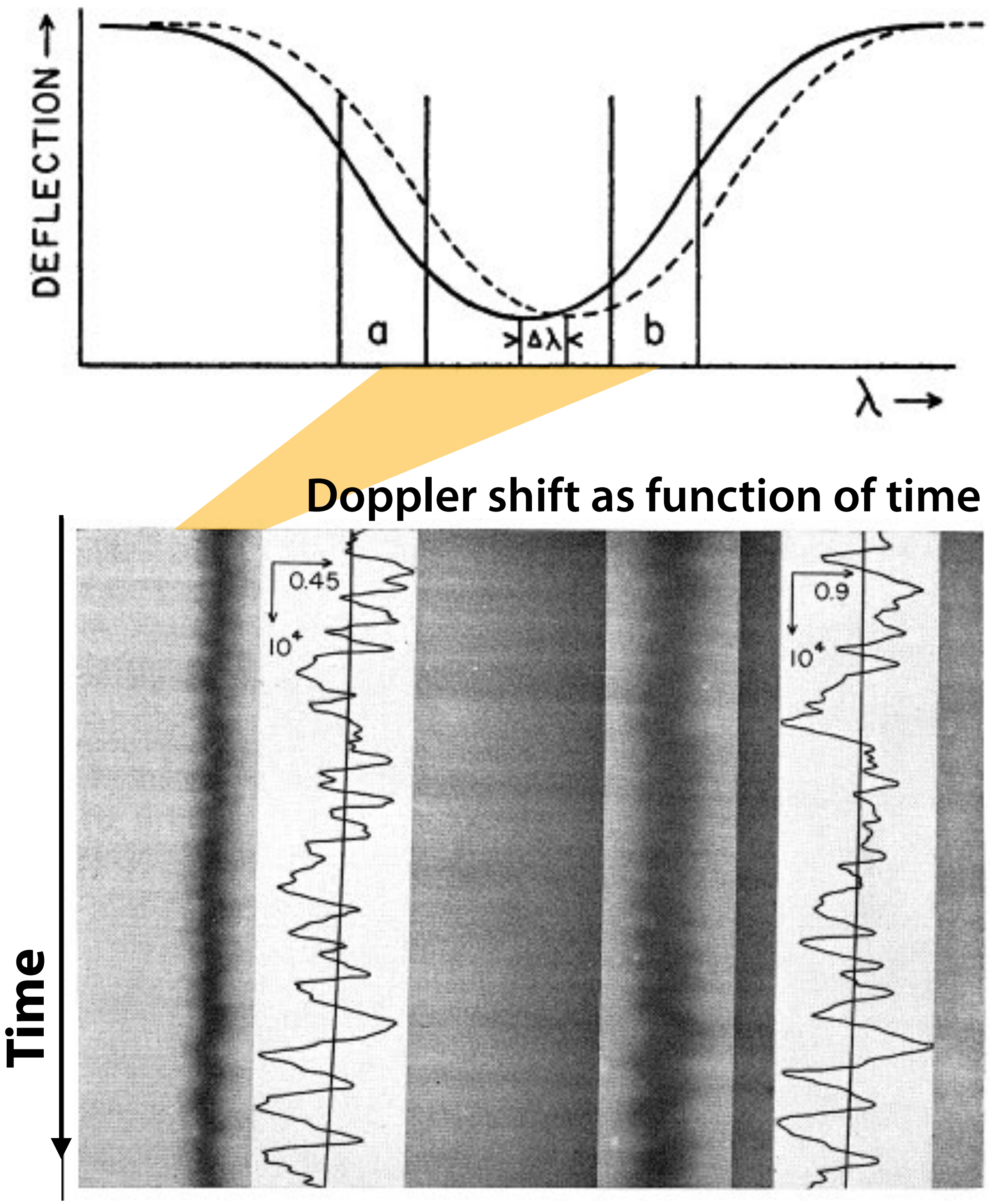

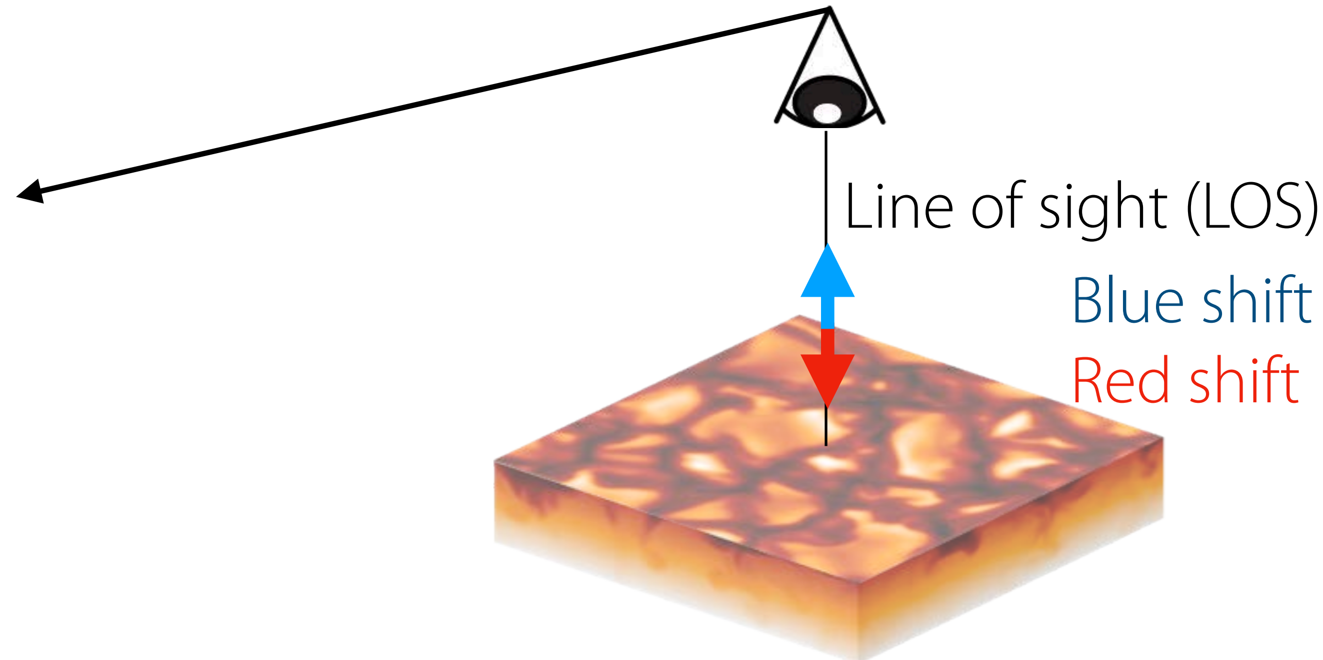

- Doppler shifts of spectral lines formed in the photosphere found to **oscillate** back and forth with **periods ~5 min**, seen allover the Sun
- Discovered in 1960 (Leighton et al. 1962)
- Also seen in the intensity itself with relative amplitudes of a few percent

Spectrum and velocity curves for the lines Mg b2 and Ti I λ = 517.37 nm, obtained at Sacramento Peak Observatory. The arrows indicate the velocity in km/s and the distance on the Sun in km. (Evans and Michard 1962)

Helioseismology

Photospheric oscillations

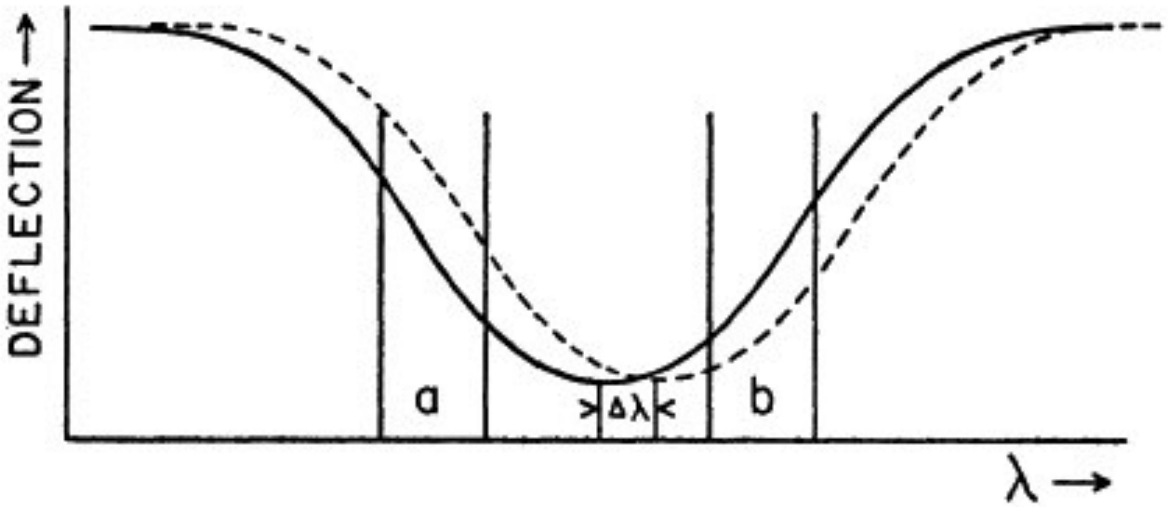

- **Doppler-difference plate:** Two spectroheliograms recorded simultaneously in the red and blue wings of a spectral line, then photographically subtracted
- Plates were scanned (over some minutes) resulting in varying time difference between the two plates…

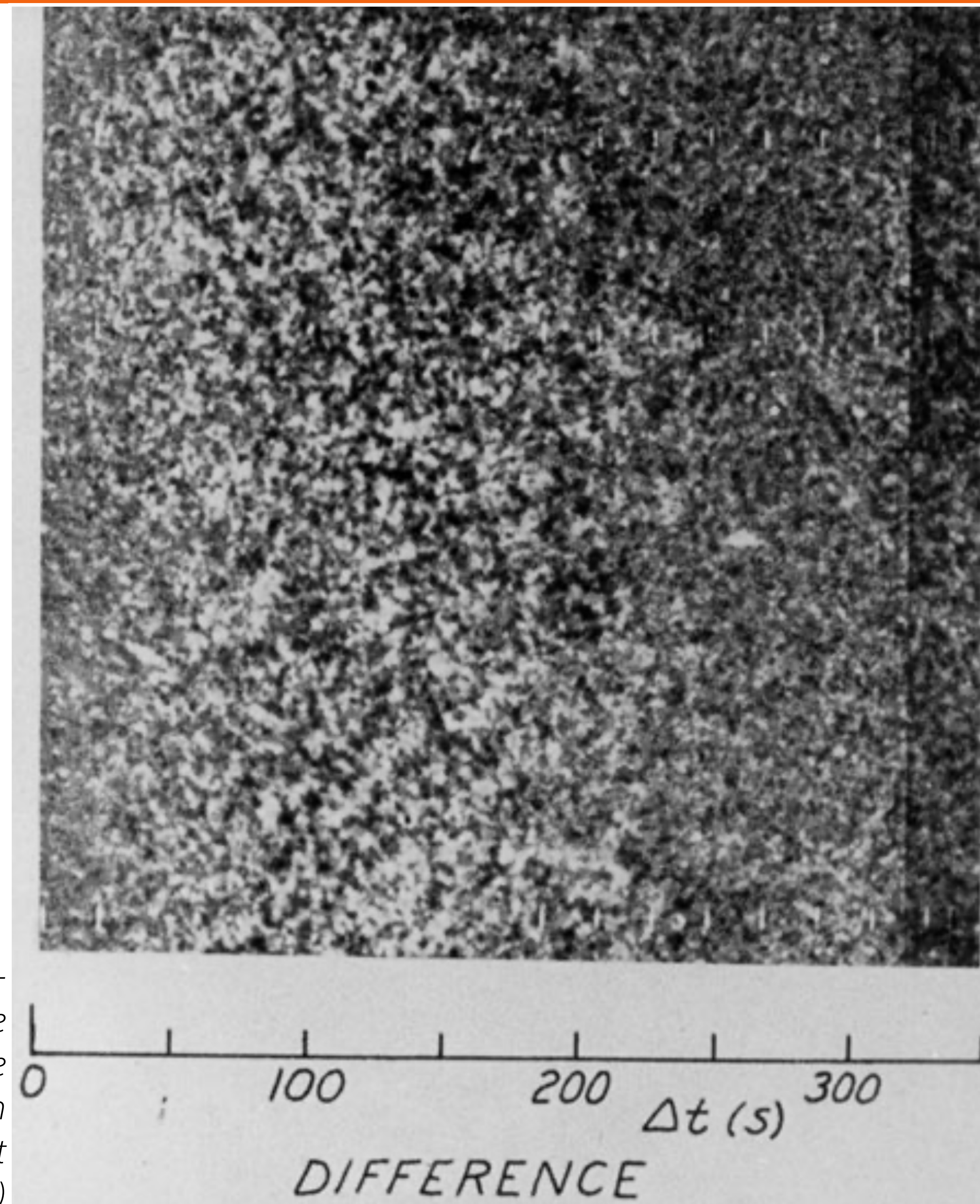

Doppler-difference plate for Ba II line λ = 455.4 nm (Leighton et al.1962)

Helioseismology

Photospheric oscillations

- Oscillations in vertical velocity
- Oscillations in photospheric lines exhibit typical velocity amplitude ~0.5 — 1 km/s, highest amplitude at a period just below ~**5min**
- Spectral lines formed here in photosphere: amplitude decreases with height
  - Max. amplitude shifts towards shorter periods higher up in the atmosphere, in the chromosphere (observed, e.g., in Hα): typically **3-min** oscillations

- **Phase difference:** Compare velocity oscillation at same location at different heights in the atmosphere (observing two different spectral lines at the same time)
- Only a small phase lag in the frequency range 2–5mHz, i.e., periods 3 — 8 min

➡ Implies a **standing wave**.

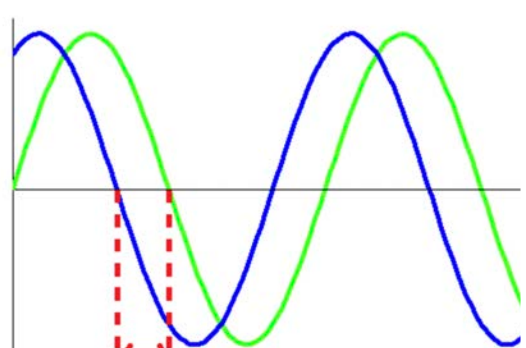

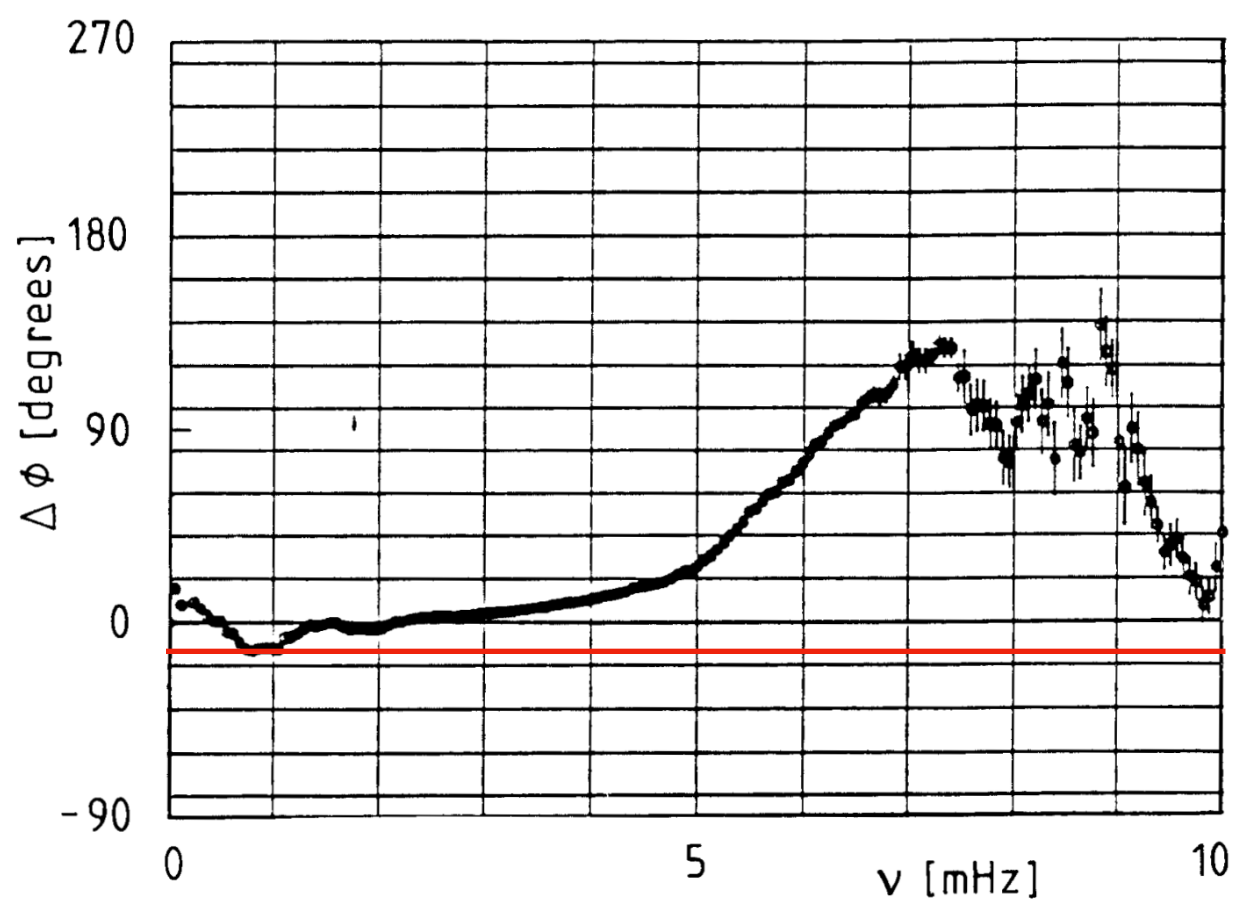

Staiger (1987)

Helioseismology

The sound of the Sun

NASA's Goddard Space Flight Center

Helioseismology

Fourier analysis — recap

- Origin of oscillations identified as acoustic waves, called **p-modes**
- Spatio-temporal properties of oscillations best revealed by **Fourier transforms**.

- Input signal (e.g. velocity) of duration t' and time resolution Δt:
  - Frequency resolution $\Delta\omega = 2\pi/t'$
  - Lowest frequency $= \Delta\omega$ (set by signal length t')
  - Highest frequency = Nyquist frequency $\omega_{\mathrm{Ny}} = \pi/\Delta t$
- To resolve two neighboring frequencies ω and $\omega + \Delta\omega$: Observation over a time span $t' = 2\pi/\Delta\omega$ needed (for the two oscillations to acquire a phase difference of exactly 2π)
- Equivalently: Variation (signal) across a distance x' with spatial resolution Δx

$$\omega = 2\pi\nu$$

$$\nu = \omega/2\pi$$

Helioseismology

Fourier analysis — recap

- The temporal and spatial scales that can be accessed from an observation are limited as

$$\Delta\omega = 2\,\pi / t' \leq \omega < \pi / \Delta t$$

$$\Delta k_x = 2\pi / x' \leq k_x < \pi / \Delta x$$

- Depends on seeing + instrumental limitations (e.g. field-of-view, angular resolution/detector pixel size etc.)
- Duration of time series ≪ duration of day from ground

➡ Long observations from space (or South Pole)

➡ GONG global oscillation network group (since late 1980ties) combing dedicated telescopes around the globe

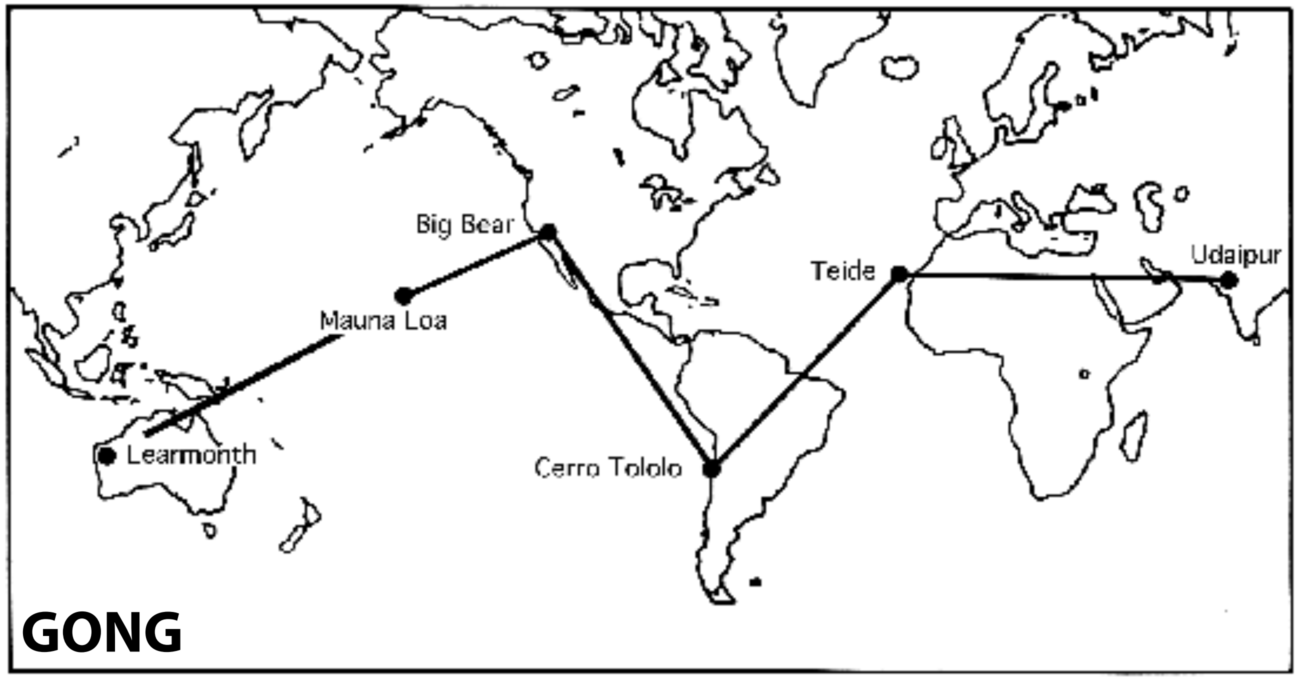

Helioseismology

Fourier analysis — recap

- Input signal = vertical velocity signal as a function of time t and position (x, y): $v\ (x,y,t)$
- **Fourier transform** f defined as

$$v(x, y, t) = \int f(k_x, k_y, \omega) \exp[\mathrm{i}(k_x x + k_y y + \omega t)]\, dk_x dk_y d\omega$$

In practice done with sums (and Fast Fourier transform)

- **Power spectrum:** $P(k_x, k_y, \omega) = f f^*$

- Note: The spatial dimensions can be collapsed into single horizontal dimension (no preferred direction here)

$$k_\mathrm{h} = (k_x^2 + k_y^2)^{1/2}$$

➡ **Power spectrum** $P(k_\mathrm{h}, \omega) = \dfrac{1}{2\pi} \displaystyle\int_0^{2\pi} P(k_\mathrm{h} \cos\phi, k_\mathrm{h} \sin\phi, \omega)\, d\phi$

Helioseismology

k-ω diagram

- Observation *v (x,y,t)*

  ➡ "2D power spectrum":
  k-ω diagram

- The p-modes show a distinctive dispersion relation!

- Important: power only in distinct **ridges:** for a given k^2 only power at certain frequencies

➡ Discrete spectrum suggests the oscillations are trapped, eigenmodes of the Sun

➡ Set by the interior structure of the Sun

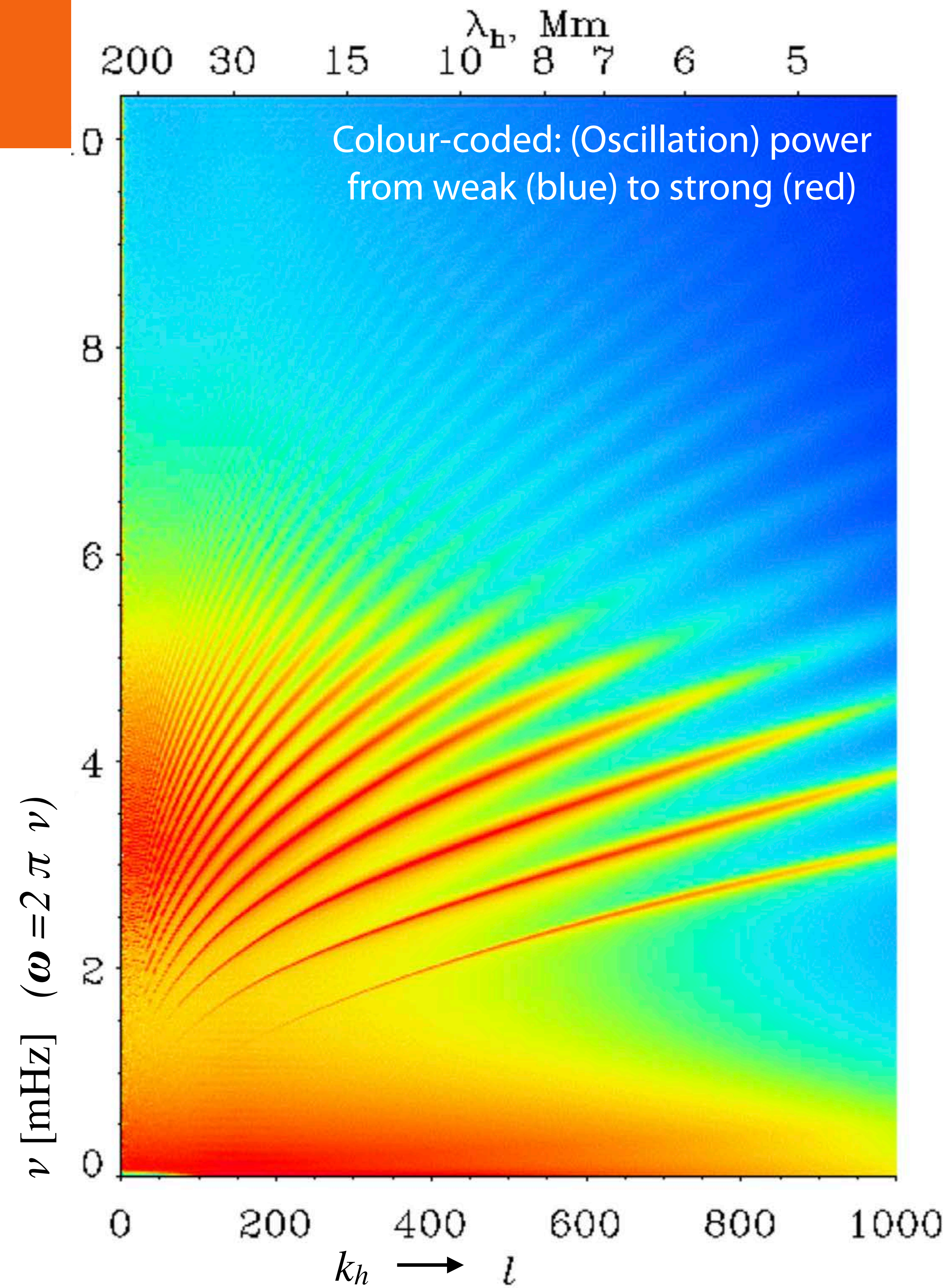

Helioseismology

k-ω diagram

- Theoretically predicted by Ulrich (1970)

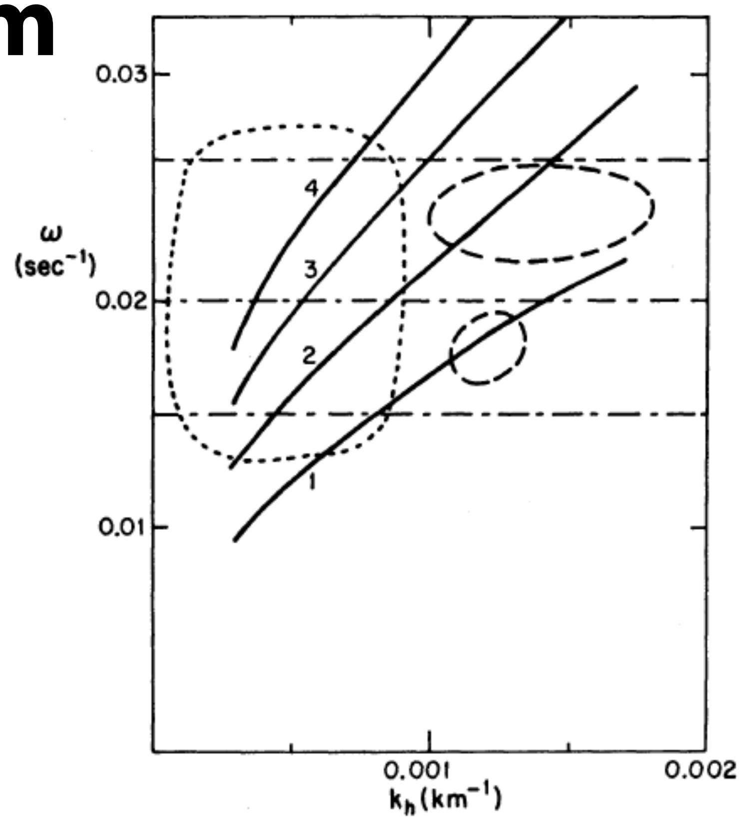

- First observed by Deubner (1974)

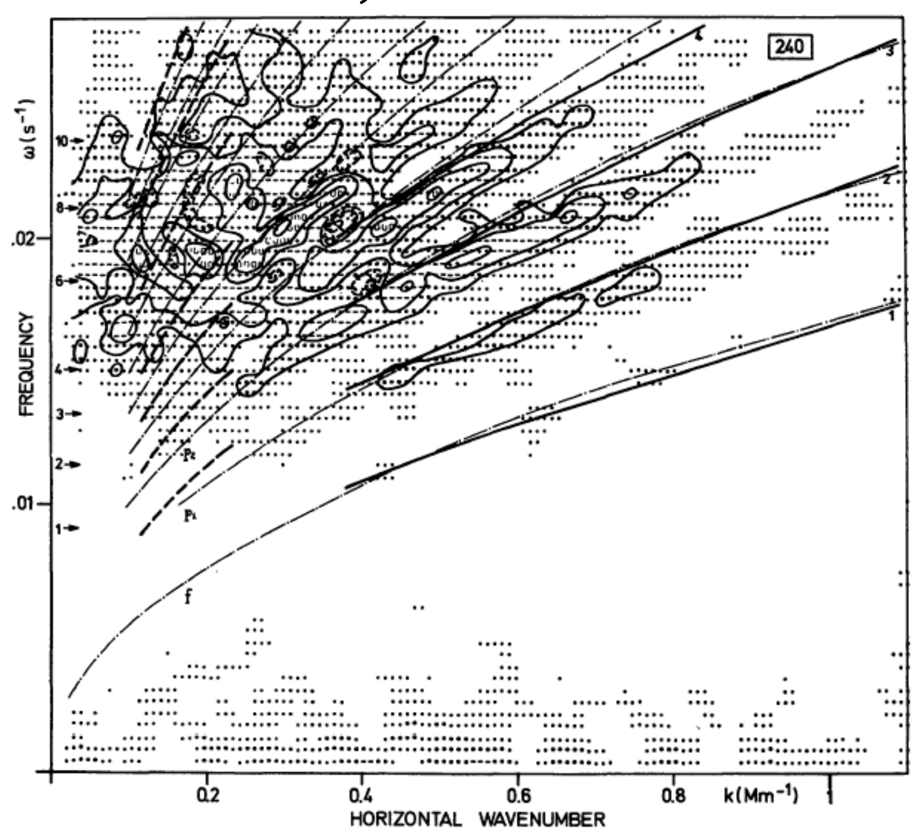

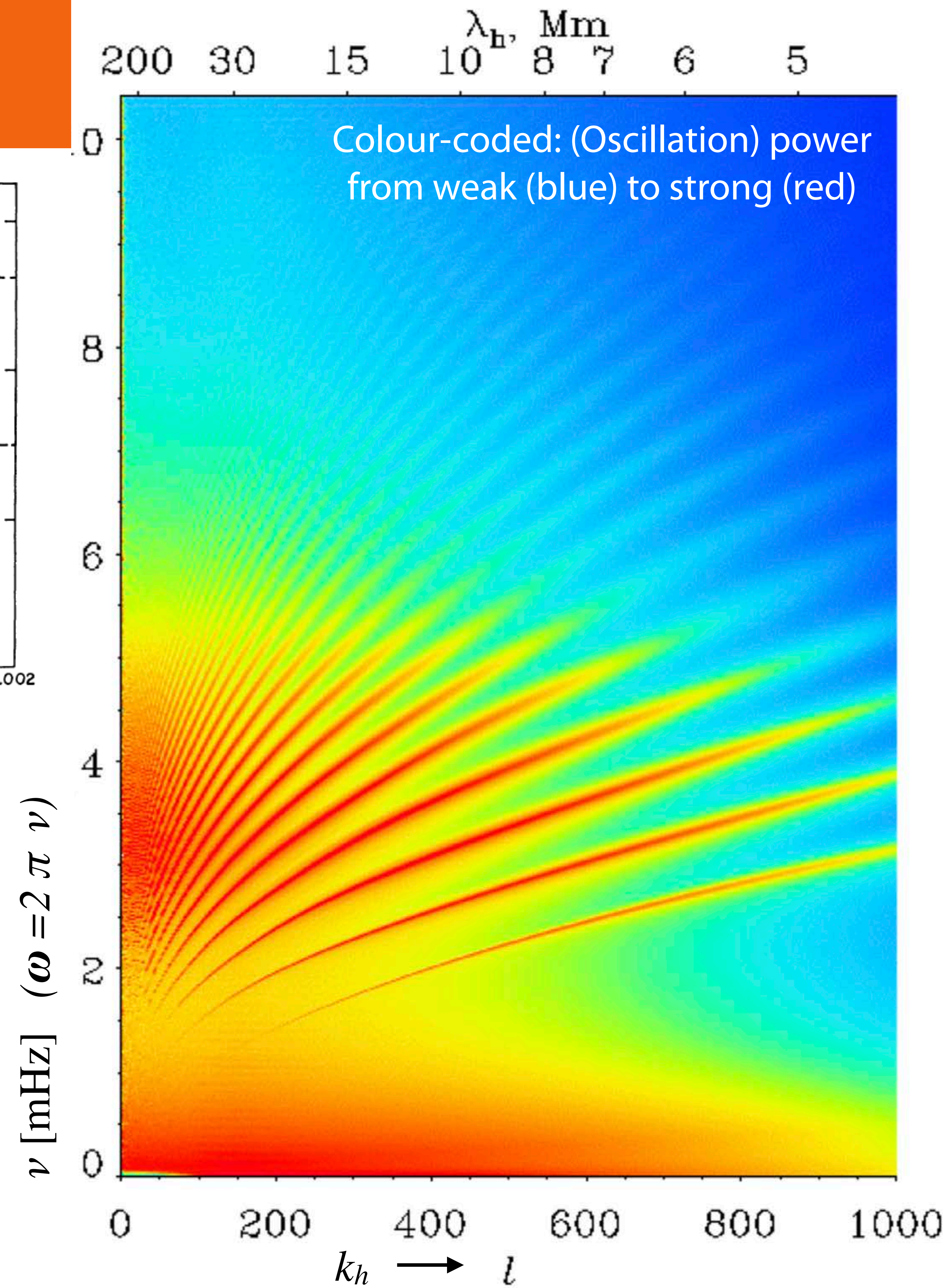

Helioseismology

Refraction & Reflection

- **Sound waves** excited and propagate through interior
- **At surface: reflection** when wavelength ~ density scale height
- Continuous spectrum of different wavelengths
- Remember: Sound speed $c_s \sim T^{1/2}$
  - ➡ Sound speed changes as function of radius
  - ➡ Sound waves get refracted
    - Shorter wavelengths refracted higher up
    - Longer wavelengths refracted deeper down

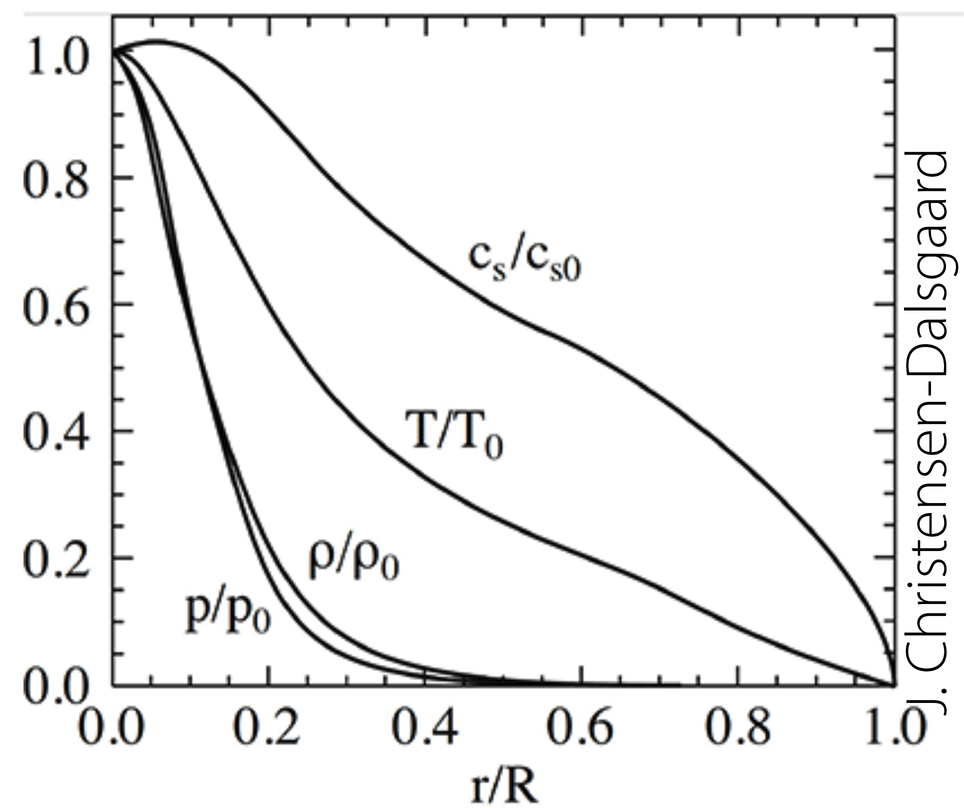

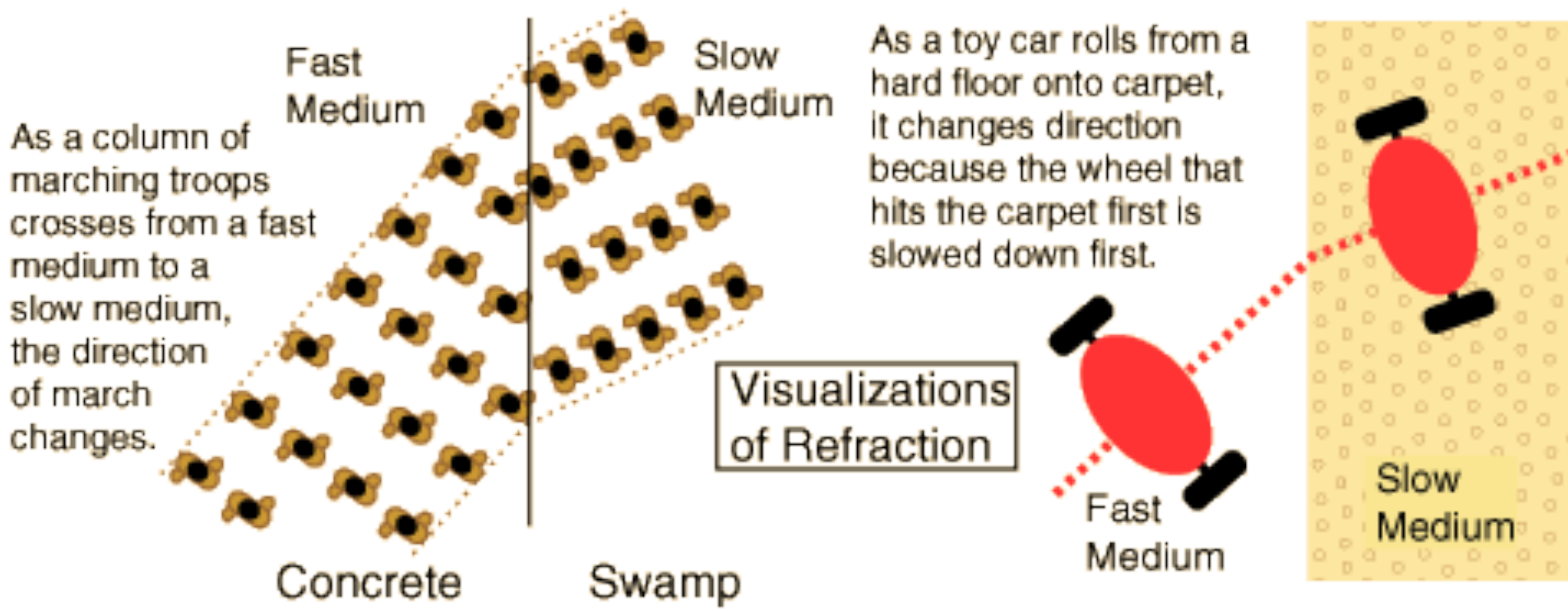

Helioseismology

Refraction & Reflection

- **Refraction**

➡ **Penetration depth of sound waves depends on their wavelength**

- Different wavelengths probe different depths
- All wavelengths together probe the stratification of the solar interior!
- Sound waves reflected at surface results in surface (patch) to oscillate up and down accordingly
- Observation and interpretation of these oscillations provides information about the interior structure of the Sun!

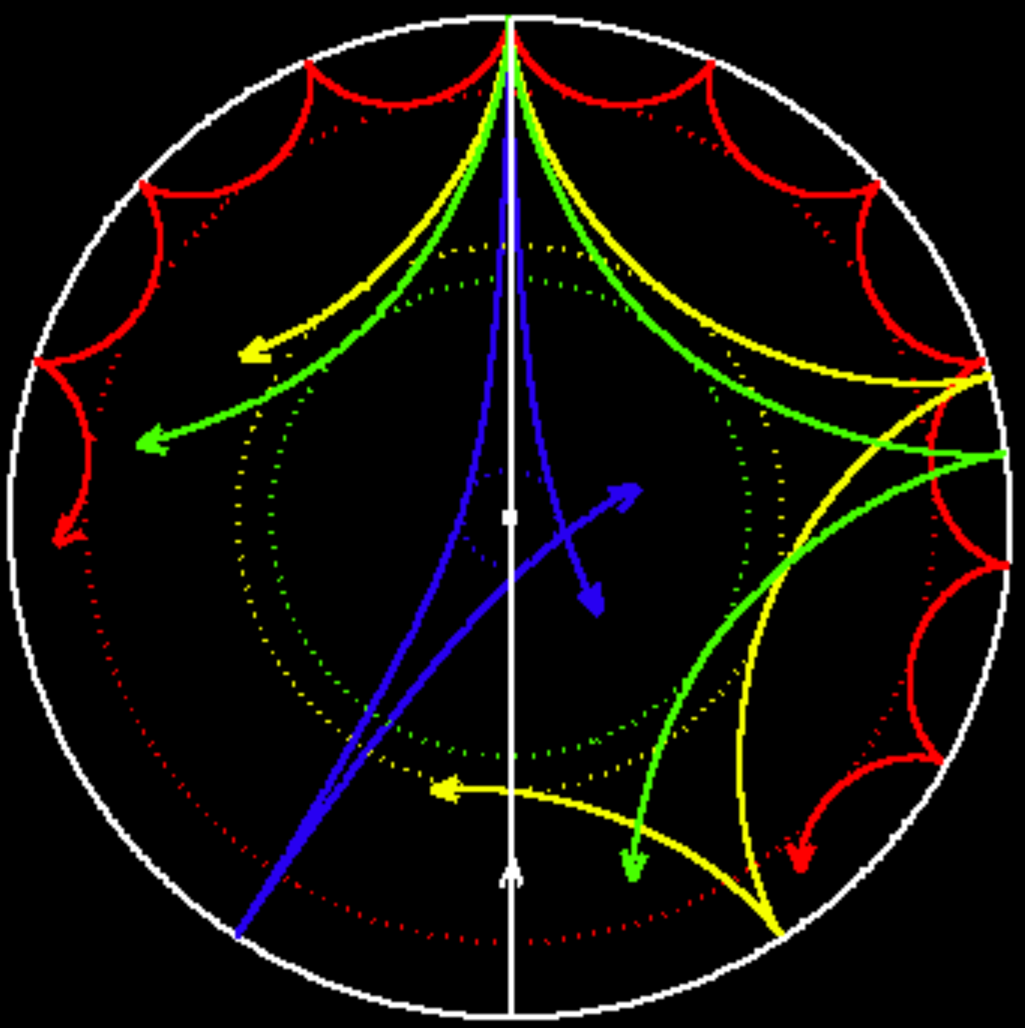

Helioseismology

Description of solar eigenmodes

- Eigen-oscillations of a sphere are described by spherical harmonics
- Each oscillation mode is identified by a set of three parameters:
  - n = number or radial nodes
  - l = number of nodes on the solar surface
  - m = number of nodes passing through the poles

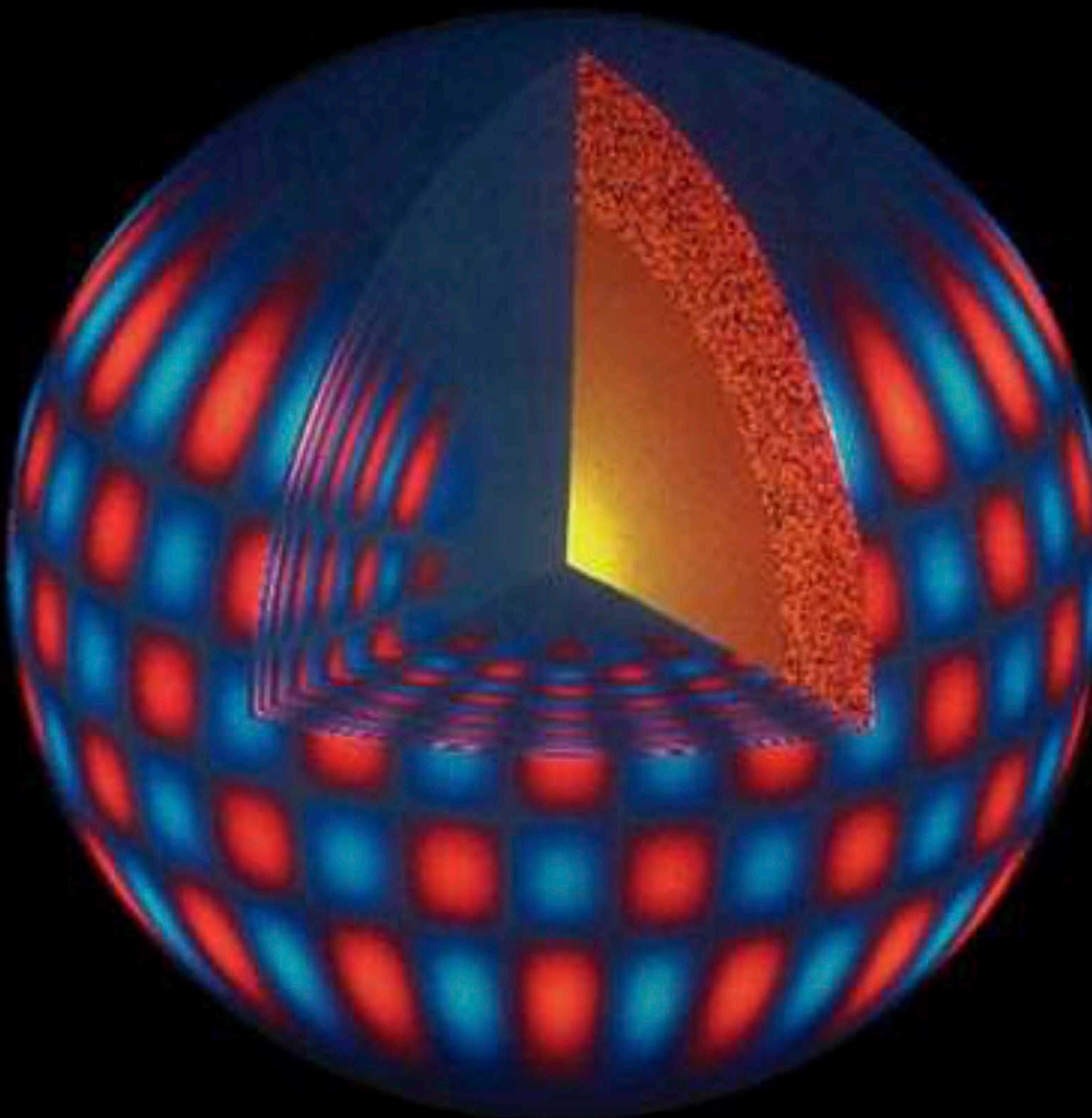

NSO/GONG

Helioseismology

Spherical harmonics

Input signal: Measured velocity signal at solar surface, no radial dependence

- So far cartesian coordinates (ok for distance « radius of the Sun)
- Better, more general: spherical polar coordinates (r, θ, ϕ): $v\ (x,y,t) \longrightarrow v\ (\theta,\phi,t)$
- Express velocity signal $v\ (\theta,\phi,t)$ now as spherical surface harmonics:

$P_l^{|m|}(\theta)$ = associated Legendre Polynomial

$$v(\theta,\phi,t) = \sum_{l=0}^{\infty} \sum_{m=-l}^{l} a_{lm}(t) Y_l^m(\theta,\phi) \quad \text{with} \quad Y_l^m(\theta,\phi) = P_l^{|m|}(\theta) e^{im\phi}$$

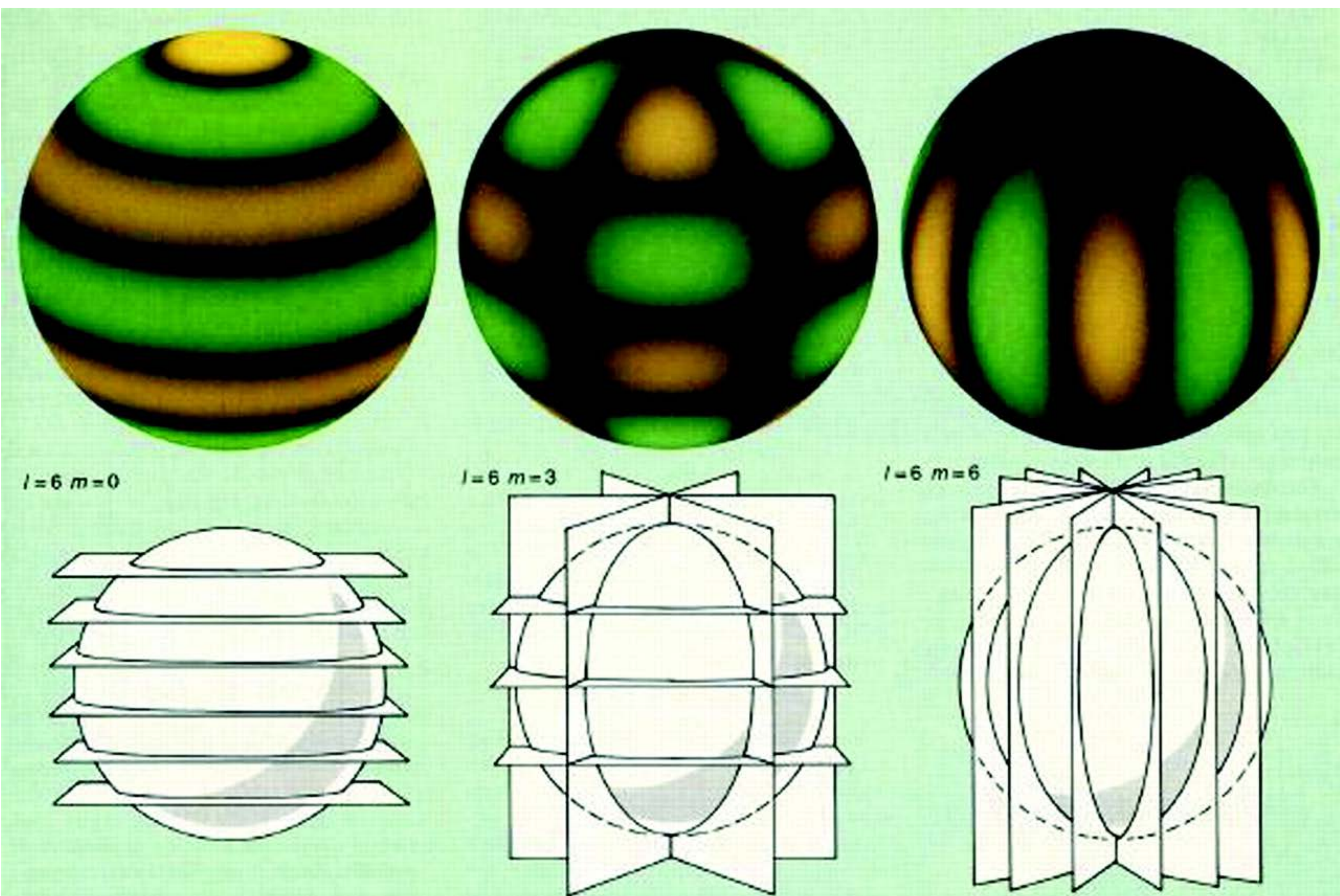

- Temporal dependence in amplitude a_{lm}
- Spatial dependence in spherical harmonic Y_l^m
- Fourier transform of amplitude a_{lm}: $F(a)$

➡ Fourier power = $F(a)F(a)^*$ (due normalisation of spherical harmonic)

- l = total number of nodes (=degree)
- m = number of nodes connecting the "poles" (=order)

Helioseismology

Spherical harmonics

- So far cartesian coordinates (ok for distance ≪ radius of the Sun)
- Better, more general: spherical polar coordinates (r, θ, ϕ): *v (x,y,t)* ⟶ *v (θ,ϕ,t)*
- Express velocity signal *v (θ,ϕ,t)* now as spherical surface harmonics:

$$v(\theta,\phi,t) = \sum_{l=0}^{\infty} \sum_{m=-l}^{l} a_{lm}(t) Y_l^m(\theta,\phi) \quad \text{with} \quad Y_l^m(\theta,\phi) = P_l^{|m|}(\theta) e^{im\phi}$$

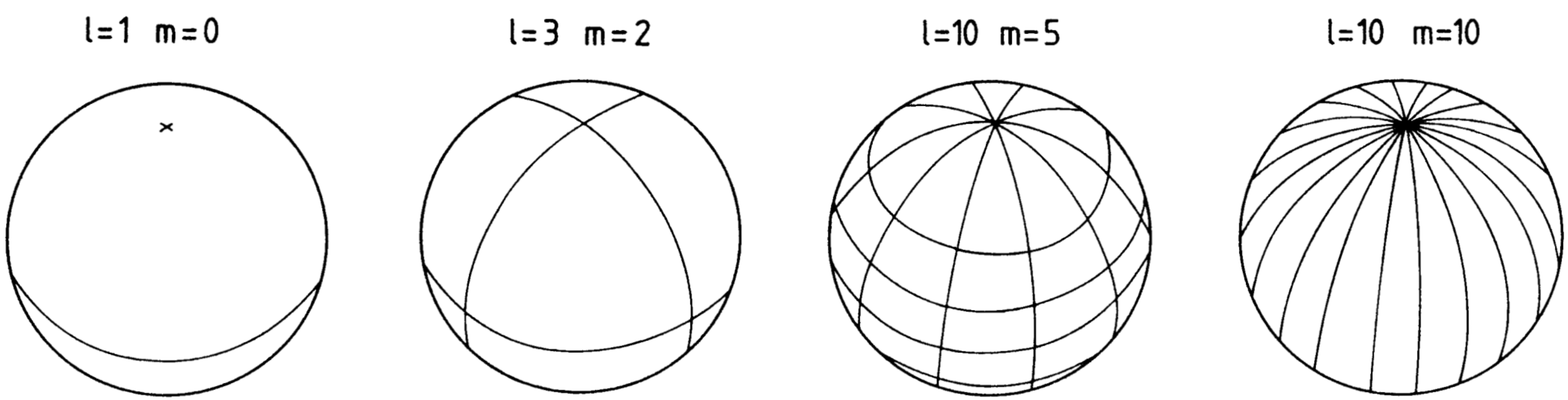

Node circles of spherical harmonics. After Noyes and Rhodes (1984)

- l = total number of nodes (=degree)
- m = number of nodes connecting the "poles" (=order)

Helioseismology

Spherical harmonics

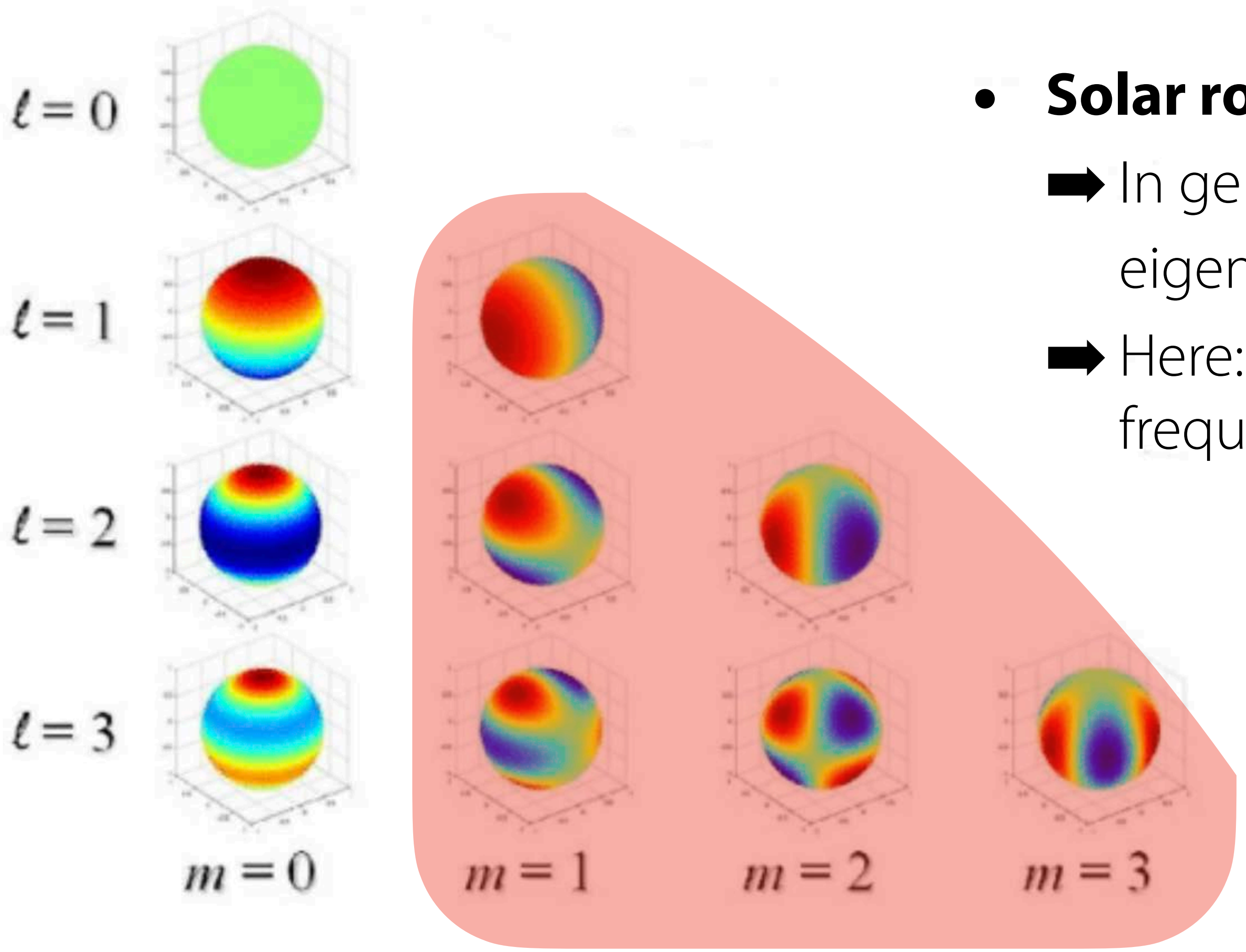

- **Solar rotation axis:**
  ➡ In general, oscillations and their eigenfrequencies would then depend on m
  ➡ Here: frequency of rotation ≪ oscillation frequencies
    ➡ Oscillation frequencies essentially independent of m.
    ➡ Simplifying assumption $m=0$

➡ The degree l of the spherical surface harmonic connected to horizontal wavenumber k_h

$$k_{\rm h} r_{\odot} = [l(l+1)]^{1/2}$$

➡ Now can evaluate the power as function of degree l and frequency ν equivalently to k-ω

Helioseismology

Interpretation of k-ω diagram

- Power ridges belong to different orders n (n = number of radial nodes)
- Power in ridge with increasing l
  ➡ Increase in frequency ν (or ω)
- Most prominent power along ridges for small n intermediate/large degree l